

THE DEVELOPMENT OF AN EXPRESSION, TO  
PREDICT THE MOVEMENT OF A  
PARTICLE IN A HYDROCLONE

By

ROBERT ELWIN BOSE

Bachelor of Science

Oklahoma State University

Stillwater, Oklahoma


1959

Submitted to the Faculty of the Graduate School  
of the Oklahoma State University  
in partial fulfillment of the requirements  
for the degree of  
MASTER OF SCIENCE  
May, 1962

NOV 6 1962

THE DEVELOPMENT OF AN EXPRESSION TO  
PREDICT THE MOVEMENT OF A  
PARTICLE IN A HYDROCLONE

Thesis Approved:

  
Thesis Adviser

  
W. H. Easton

  
Dean of the Graduate School

504270

## ACKNOWLEDGMENTS

I would like to take this opportunity to thank those who helped make this thesis possible.

Acknowledgment is given to Dr. J. H. Boggs, Head of the School of Mechanical Engineering, for the research assistantship which I have held while attending Oklahoma State University. I wish to thank Professors E. C. Fitch, Jr. and W. H. Easton for reviewing and commenting on this thesis and for their assistance throughout the Master of Science degree program.

Special acknowledgment is given to Richard Gerlach for his assistance in the derivation of equations and experimental tests.

To Michael Zaloudek and Roger Tucker for their help and assistance while working on this research project with me.

Recognition is given to Professor Bert S. Davenport and Technicians John A. McCandless and George Cooper for their assistance.

## TABLE OF CONTENTS

Chapter	Page
I. INTRODUCTION . . . . .	1
II. PREVIOUS INVESTIGATION . . . . .	4
III. STATEMENT OF PROBLEM . . . . .	18
IV. ANALYTICAL DEVELOPMENT AND ANALOG COMPUTER RESULTS . . . . .	19
V. EXPERIMENTAL VERIFICATION . . . . .	31
VI. CONCLUSIONS . . . . .	44
VII. RECOMMENDATIONS FOR FUTURE STUDY . . . . .	46
SELECTED BIBLIOGRAPHY . . . . .	47
APPENDIX . . . . .	48
A. Scaling of the Analog Computer . . . . .	48
B. List of Symbols and Abbreviations . . . . .	53
C. Operation and Principle of Particle Counter . . . . .	57
D. Apparatus and Equipment . . . . .	61

## LIST OF TABLES

Table	Page
I. Particle Radius . . . . .	30
II. Function Generator Data . . . . .	52
III. Coulter Counter Data . . . . .	60

## LIST OF FIGURES

Figure	Page
1. Hydroclone Flow Patterns . . . . .	2
2. Hydroclone Velocity Profiles . . . . .	9
3. Velocity Fields (A), (B), (C), and (D) . . . . .	11
4. Radial and Tangential Velocity Fields . . . . .	13
5. Forces Acting on Spherical Particle . . . . .	20
6. Hydroclone Radius Versus Flow Rate Plot . . . . .	28
7. Hydroclone Dimensions . . . . .	32
8. Hydroclone Components . . . . .	34
9. Power Stand . . . . .	35
10. Electrical Schematic for Power Stand . . . . .	36
11. Hydraulic Schematic for Power Stand . . . . .	37
12. 0.500 Inch Radius Hydroclone Separation Efficiency Plots . . . . .	39
13. 0.281 Inch Radius Hydroclone Separation Efficiency Plots . . . . .	40
14. Comparison of Experimental and Analog Computer Results . . . . .	42
15. Problem Board Schematic . . . . .	50
16. Function (r) Plot . . . . .	51
17. Coulter Counter Schematic . . . . .	59

## CHAPTER I

### INTRODUCTION

During recent years, the hydroclone, sometimes referred to as a cyclone, has been applied for use in many fields where liquid-solid separation is required. In each application, use has been made of the high particle-settling velocities which result from forces that occasionally reach a value of several thousand times the force due to gravity. Unlike a filter, a hydroclone does not utilize an obstruction to clean fluid. It is simple in construction and relatively inexpensive. Although hydroclones have high flow rate capacity, pressure drop does present a problem when a high capacity flow rate and a high separation efficiency is demanded. A brief description of the design and flow patterns will familiarize the reader with the operation of the hydroclone.

The hydroclone, shown in Figure 1, consists of a cylindrical section (A), mounted above a truncated cone (B), with an inlet nozzle (C), that enters tangentially into the top of the cylindrical section. The apex of the truncated cone serves as the underflow nozzle (D), and a tube extended partially into the center of the cylindrical section

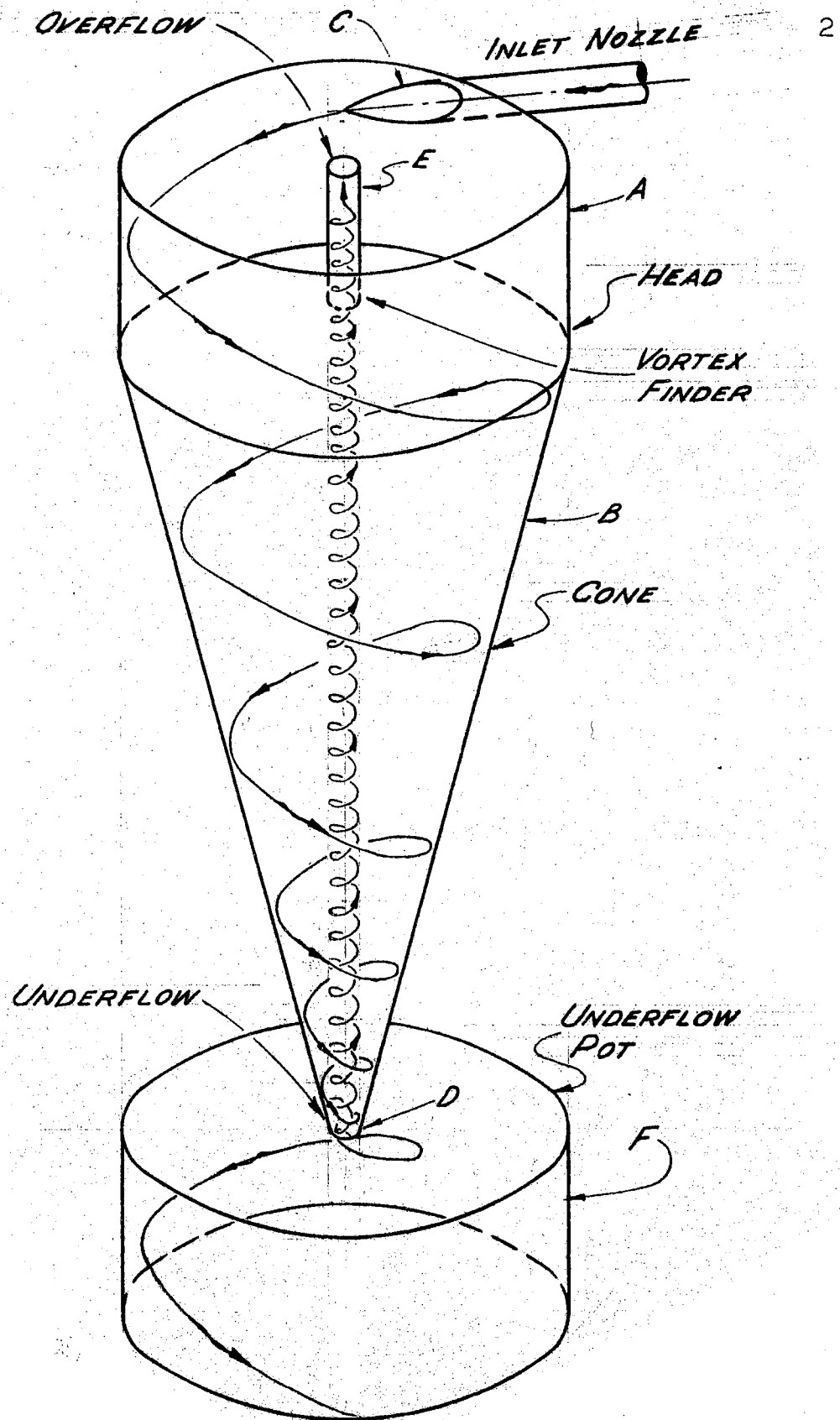


Figure 1. Hydroclone Flow Patterns



from the top of the hydroclone serves as an overflow nozzle (E). An underflow pot (F), is located at the apex of the cone section to collect particles that are discharged from the underflow nozzle. The flow patterns in the hydroclone, shown in Figure 1 (page 2), consist of a free vortex generated by the radial movement of the fluid. The fluid enters tangential to the cylindrical section creating a spiral of high centrifugal force. Because of this high centrifugal force, the particles of sufficient size and gravity are moved outward and are spirally discharged through the apex of the cone or the underflow nozzle. However, most of the fluid moves radially inward, thus generating a forced vortex which is discharged at the top of the cylindrical section or the overflow nozzle.

One of the major advantages of a hydroclone is that the underflow pot has the capability of collecting large amounts of contaminant before the pot has to be cleaned. Unlike the hydroclone, a filter element is replaced after a small amount of contaminant is collected and then cleaned by chemical, sonic or other methods. A hydroclone may be used in a hydraulic system in front of a filter to remove 100 per cent of all large particles and 95 per cent or more of the smaller particles, thus increasing the life of the filter by reducing the amount of contaminant it has to collect.

## CHAPTER II

### PREVIOUS INVESTIGATION

Although the hydroclone has been widely used over the past half century, its use in removing contaminant from hydraulic oil is a relatively new idea. Until recently, the main use of the hydroclone was to classify coal from water by the removal of the larger particles through the underflow nozzle and the smaller particles through the overflow nozzle. Modern applications have used the hydroclone to separate fission particles and corrosion products from atomic reactors. The majority of investigators rate a hydroclone by its separation efficiency rather than on an absolute basis because until recently the hydroclone was used only for classifying particles.

The most common separation efficiency rating is the  $d_{50}$  point. The  $d_{50}$  point is defined as the point at which the hydroclone allows 50 per cent by weight of a specific micron size particles to pass through the underflow nozzle and 50 per cent of the particles to pass through the overflow nozzle. Matschke and Dahlstrom (1) have proven that the empirical equation,

$$d_{50} = \frac{C(D_o D_f)^{0.65}}{(GPM)^{0.60}} \left[ \frac{1}{(\rho_S - \rho_L)} \right]^{0.50} \quad (2-1)$$

can be used to predict closely the solid elimination efficiency of a miniature hydroclone. The above authors also have stated that, for proper cyclone design with small diameter hydroclones, the largest particle size found in the overflow fluid will be approximately twice the size of the  $d_{50}$  value for similar specific gravities. Haas, et al. (2), has suggested that the expression,

$$d_{50} = \frac{C D_C^{0.5} \mu^{0.5}}{\Delta P^{0.25} (\rho_S - \rho_L)^{0.5}} \quad (2-2)$$

can be used as a rough estimate of the separation efficiency. Although this equation was based on certain assumptions and was not developed from experimental data, it does indicate the possible influence of viscosity which might be useful in predicting separation efficiency of hydroclones. Dahlstrom (3) has developed an empirical equation for the flow capacity correlation,

$$\frac{Q}{(\Delta P)^{0.5}} = k(D_o D_f)^{0.9}, \quad (2-3)$$

which can be used for almost any diameter hydroclone. The term,  $\frac{Q}{\Delta P^{0.5}}$ , has been designated as the capacity ratio and is the basic expression for any hydroclone or flow apparatus, i.e., capacity is a function of the square root of energy loss and should remain constant for any constant dimension apparatus. Haas, et al. (2), has developed an equation

which is optimized for hydroclones of one inch or smaller and is as follows:

$$\frac{Q}{(\Delta P)^{0.44}} = k D_C^{1.8} . \quad (2-4)$$

A more generalized expression developed by Yoshioka and Hatta (4) includes the hydroclone inlet diameter, overflow diameter, and cyclone diameter and is as follows:

$$\Delta P = \frac{k Q^2}{D_C^{0.9} D_f^{1.2} D_o^{1.9}} . \quad (2-5)$$

The constant,  $k$ , in all three of these flow capacity correlations is a function of the included angle of the cone section, distance between conical section and vortex finder, surface finish, and type of underflow discharge. Moder (5) has recommended that  $k$  should equal 5.61 for a  $20^\circ$  cone with no cylindrical section and should be increased 6 to 8 per cent with a cylindrical section. For  $15^\circ$  included angles,  $k = 6.38$  is recommended.

Moder (5) has pointed out that the tangential velocity in the forced vortex can be expressed by the general expression  $V_t = \frac{k''}{r^n}$  in regions outside the central core. The value of  $n$  for a non viscous fluid is equal to 1 when the law of conservation of angular momentum applies. As long as the total energy of the system remains constant, the product  $V_t r$  must be constant. The value of  $n$  for a very viscous fluid would equal -1 for the case in which constant

angular velocity applies. Many investigators have used values of  $n$  from  $-1$  to  $1$  in their studies. A value of  $0.5$  or less would be expected for a liquid cyclone due to larger viscous forces.

Dreissen (6), with the assumption that the flow in a cyclone can be compared to a two dimensional vortex (flat) in an incompressible viscous medium, applied the equations of Navier-Stokes in polar coordinates and simplified the equations to the following expressions:

$$\frac{E^2}{(2\pi)^2 r^3} + \frac{V_t^2}{r} = \frac{1}{\rho} \frac{dP}{dr} \quad (2-6)$$

and

$$V_t = \frac{c}{n' + 1} r^{n'} + \frac{c_1}{r} \quad (2-7)$$

where

$$n' = 1 - \frac{E}{2\pi v} \quad (2-8)$$

The logarithmic solution was obtained when  $n'$  was given the value of  $-1$ . The constants,  $c$  and  $c_1$ , were evaluated from the boundary conditions of  $V = V_2$  at  $r = r_2$  and  $\frac{dv}{dr} = 0$  at  $r = r_1$  and the expression for the tangential velocity obtained is as follows:

$$V_t = \frac{V_2 r_2}{r} \left[ \frac{1 + \ln \frac{r}{r_1}}{1 + \ln \frac{r_2}{r_1}} \right] \quad (2-9)$$

The tangential velocity can be expressed as  $V_t = k'r$  in the central core or the forced vortex. It is evident that the tangential velocity reaches a maximum value in the vicinity of the vortex finder radius (Figure 2). Kelsall (7) has proven by probing the tangential velocity field that the position of this maximum value is independent of the overflow diameter.

Moder (5) has shown that the principal acceleration of the hydroclone is the result of the tangential velocity. This acceleration caused by the tangential velocity can be expressed numerically by  $V_t^2/r$ . The changes in the radial and axial velocities are not large enough to change the effect of  $V_t^2/r$ . In the main vortex, the particles are moved toward the central core by the radial velocity but are retarded by the acceleration term  $V_t^2/r$ . Therefore, a particle would find a radius at which the settling velocity, relative to the fluid, equalled the radial fluid velocity. The particle would then rotate about the axis at this equilibrium radius. Since the centrifugal force is proportional to  $V_t^2/r$  and  $V_t$  is proportional to  $1/r$ , the centrifugal force is proportional to  $1/r^3$ . The particles are also subjected to a centripetal force arising from the viscous drag of the particle. This force is proportional to the radial velocity, according to Stokes' Law and, therefore, is proportional to  $1/r$ . It is at the intersection of these curves that the equilibrium radius exists and the particle rotates about this axis (Figure 2).

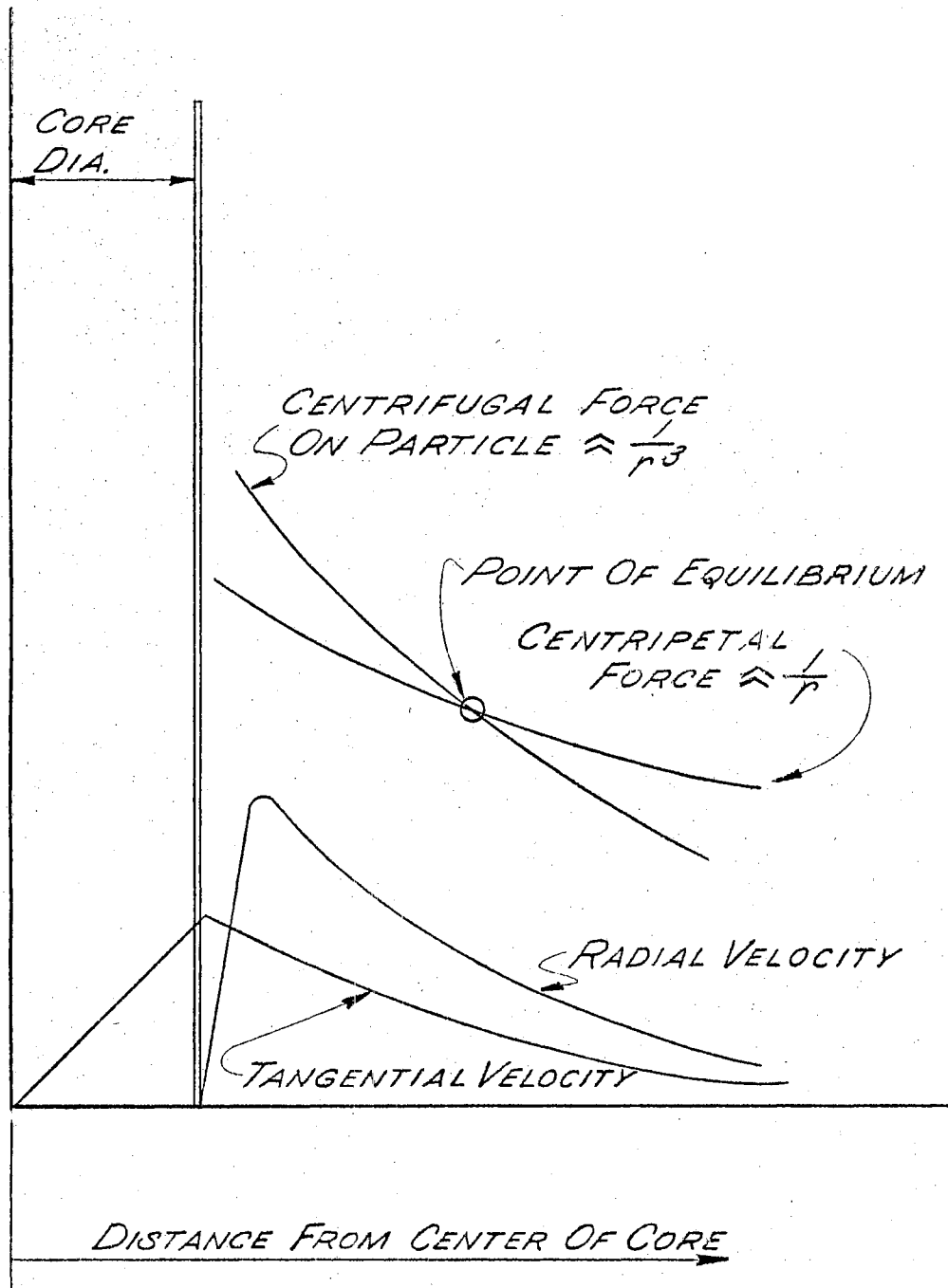


Figure 2. Hydroclone Velocity Profiles

Criner (8) has presented a paper showing the various velocities and different flow patterns in the hydroclone. Because the flow is introduced tangentially, a vortex type flow (flow A, Figure 3) must exist at every axial cross section. Since this fluid is introduced at the outer wall of the hydroclone and is removed through the inner vortex, there must exist a velocity perpendicular to the hydroclone axis. This radial velocity provides the necessary energy to the inner regions to replace that energy which is dissipated by the turbulence and is necessary to maintain the vortex strength. Due to this radial velocity that occurs when the fluid is initially introduced into the hydroclone, flow B occurs (Figure 3). This flow pattern, B, is one of the causes of short circuiting that occurs in the hydroclone. Flow C (Figure 3), according to Moder (5), is the result of the high resistance encountered at the cone apex. The resistance caused by boundary effects is unimportant in the upper cylindrical section and upper part of the cone. But, because of the small area at the hydroclone cone apex and large tangential velocity, the flow resistance and energy dissipation in the boundary layer is relatively higher than other regions of the cyclone. Therefore, other fluid must reach this area in order to supply these losses and, consequently, flow C exists. The effect of flow C is to increase the radial velocity near the overflow nozzle and decrease the radial velocity in the upper part of the cone. However, it is only at the very



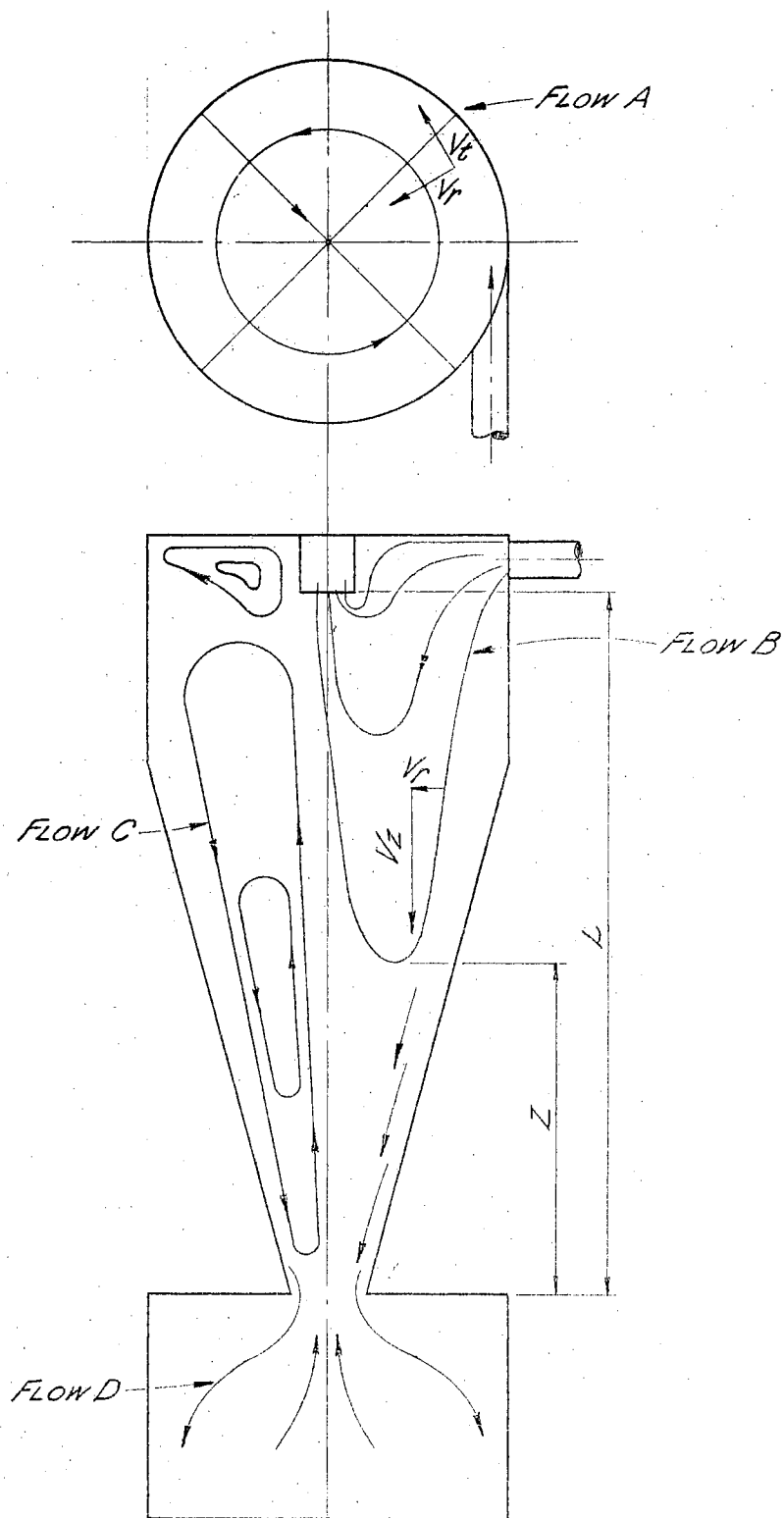
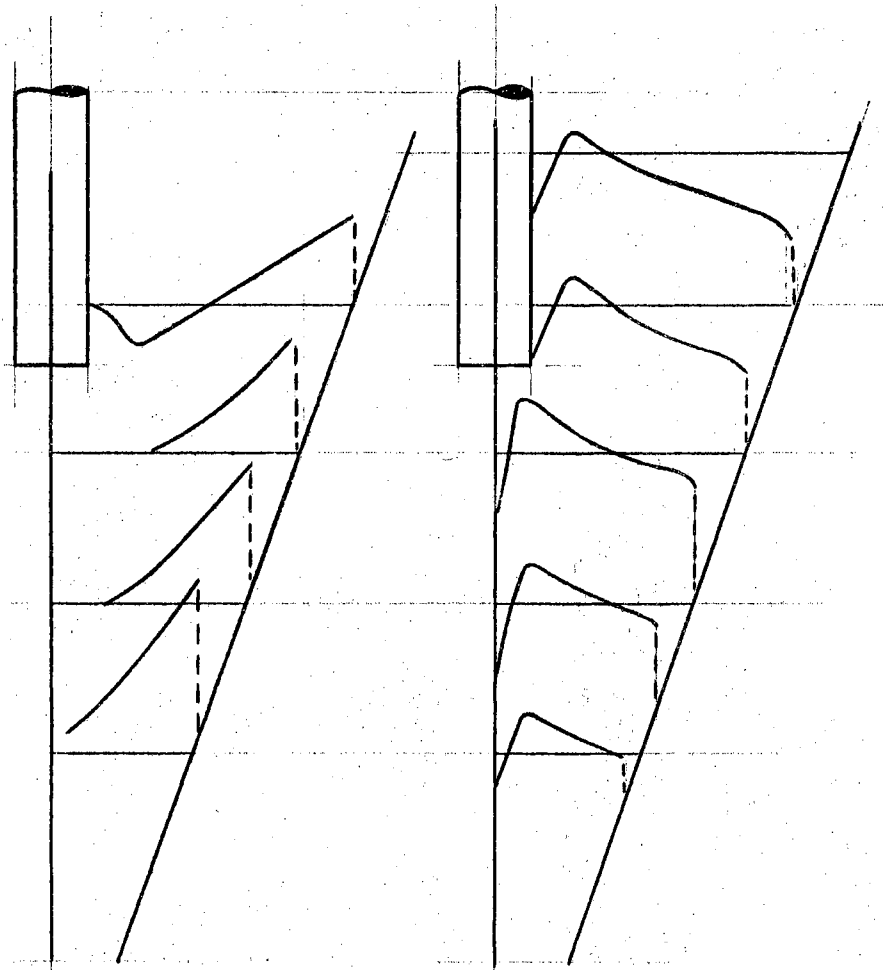


Figure 3. Velocity Fields (A), (B), (C), and (D)

tip of the cone that the radial velocity deviates from the average value.

Kelsall (7) has shown that two secondary flows exist, one involving recirculation of liquid and solid particles above the vortex finder and the other a short circuit flow down the outside wall of the vortex finder. These flows were noted by observing fine aluminum particles with ultra-microscope illumination and a microscope fitted with rotating objectives. It is believed that the majority of coarser particles that are discharged through the overflow nozzle are a result of the short circuit path or flow B. Therefore, the vortex finder should be of sufficient length to provide the necessary time for the fluid to pick up the particle and, as a result of the centrifugal acceleration of the fluid, to move the particle to the wall so that it will be removed at the underflow. The finer particles found in the overflow are believed to be a result of flow pattern C. Because of the high vertical velocity near the inner vortex, the finer particles being carried in by the radial movement of the liquid are carried upward in the direction of the vortex finder. As the radial velocity at any radius decreases as the bottom of the vortex finder is approached and the centrifugal acceleration at this radius remains unchanged (Figure 4), these finer particles are moved outward again. Therefore, the length of the vortex finder should be decreased so that the time for the particles to move outward again is increased.



(a) FLUID RADIAL VELOCITIES (b) FLUID TANGENTIAL VELOCITIES

\*Curves plotted from a common reference line.

Figure 4. Radial and Tangential Velocity Fields

Haas, et al. (2), has suggested that an underflow pot be used to collect particles that are spirally discharged at the underflow nozzle. The particles that are discharged through the underflow nozzle are moved out to the walls by the existing centrifugal force on the particles and flow down along the walls of the hydroclone pot. An equal volume of fluid returns through the overflow nozzle by means of the forced vortex path (Flow D, Figure 3, page 11). The settling out of the particles in the underflow pot could improve the efficiency of the hydroclone. However, the above authors state that, because of their size, the smaller particles might not settle out as a result of thermal currents.

Criner (7) has developed an expression that locates the position at which all flow is discharged through the underflow nozzle. This plane, perpendicular to the hydroclone axis, is referred to as the "Plane of No Return" and is given by

$$Z = L \frac{Q}{Q_u} \quad (2-10)$$

A wide variety of devices have been employed or proposed by Shepherd and Lappel (9) to improve collection efficiency or reducing pressure drop. Straightening vanes located in the vortex finder, straightening vanes on a baffle below the vortex finder, and a helical roof were some of the more common devices used for reducing the pressure drop.

The underflow nozzle is perhaps the most important of the variables in a cyclone, especially if maximum separation efficiency is required. If the underflow nozzle is too large, the pot will contain a large amount of circulating fluid which could cause it to pick up particles and to return them to the overflow nozzle. To prevent this, the opening should be as small as possible and still large enough to allow the largest particles encountered to be discharged into the underflow pot.

A brief summary of geometric guides for design purposes was given by Matschke and Dahlstrom (1) as follows:

1. Cyclone included angle should be kept as low as possible (between 10 and 20 degrees).
2. The bottom of the vortex finder should be 6 inches or one cyclone diameter, whichever is less from the transition point between the conical section and cylindrical sections.
3. The vortex finder should extend just below the bottom of the inlet nozzle to the cyclone.
4. Inlet angle should allow the entering fluid to descend at least one inlet nozzle diameter in the first revolution.
5. Inlet, overflow, or vortex finder dimensions are determined with respect to cyclone diameter according to the following equations:

$$\frac{2D_f + D_o}{D_c} = 0.35 \text{ to } 0.70$$

$$\frac{D_o}{D_f} = 1.0 \text{ to } 1.6 \quad (2-11)$$

6. Distance between the top of the inlet port and cyclone top should be kept at a minimum to minimize secondary flows that result in an overall decrease in efficiency.

Two different differential equations that describe the motion of a particle in a hydroclone have been developed in theses written by Gilbert (11) and Beattie (12) at Oklahoma State University. The drag term in each equation was assumed to be the result of the particle being accelerated through the fluid as it moved to the outer wall and the effect of the radial movement of the fluid was neglected. However, the fluid is at or near the outer wall when initially introduced into the hydroclone. Therefore, these expressions have predicted that many particles of insufficient size or density will be removed. This discrepancy is due to the fact that the inward radial movement of the fluid was neglected. This inward radial movement of the fluid could, however, carry the particle from the wall to the inner vortex if the drag force due to the radial movement of the fluid exceeded the centrifugal force of the particle. In only one of these theses was an experimental study performed to determine hydroclone efficiency. Downstream samples were taken and filtered through millipore paper to collect any particles that the hydroclone had not separated. The particles on the filter paper were then counted by using a microscope with a micrometer stage eyepiece. The actual number of particles could not be counted accurately because they were either transparent or too

small to be seen with the eye using the microscope. As a result of this difficulty, very little qualitative information was gained about actual hydroclone efficiency.

### CHAPTER III

#### STATEMENT OF PROBLEM

The objective of this study was to develop an expression to predict the separation efficiency of a hydroclone. This expression was solved on the analog computer varying the flow rate, hydroclone radius, and particle diameter. The results from the analog computer were used to plot curves of hydroclone radius versus flow rate for constant particle diameters.

Several hydroclones were built and tested to verify the analytical expression. Samples of the fluid before and after the hydroclone were taken to determine the separation efficiency at different flow rates. An electronic particle counter was used to check the samples in order to determine the separation efficiency.



## CHAPTER IV

### ANALYTICAL DEVELOPMENT AND ANALOG COMPUTER RESULTS

From previous investigation, it was shown that the forces on a particle in a hydroclone were of two kinds, the centrifugal force and the viscous drag force. Therefore, the basic assumption will be that the force of acceleration is equal to the centrifugal force minus the drag force (Figure 5) or

$$F_a = F_c - F_d \quad . \quad (4-1)$$

The force of acceleration is equal to the product of the mass of the particle and the radial acceleration and for a spherical particle is given by

$$F_a = \frac{4}{3}\pi R^3 \rho_s \frac{dV_r}{dt} \quad . \quad (4-2)$$

The centrifugal force is equal to the product of the relative mass of the particle and the radial acceleration and for a spherical particle is given by

$$F_c = \frac{4}{3}\pi R^3 (\rho_s - \rho_L) \frac{V_t^2}{r} \quad . \quad (4-3)$$

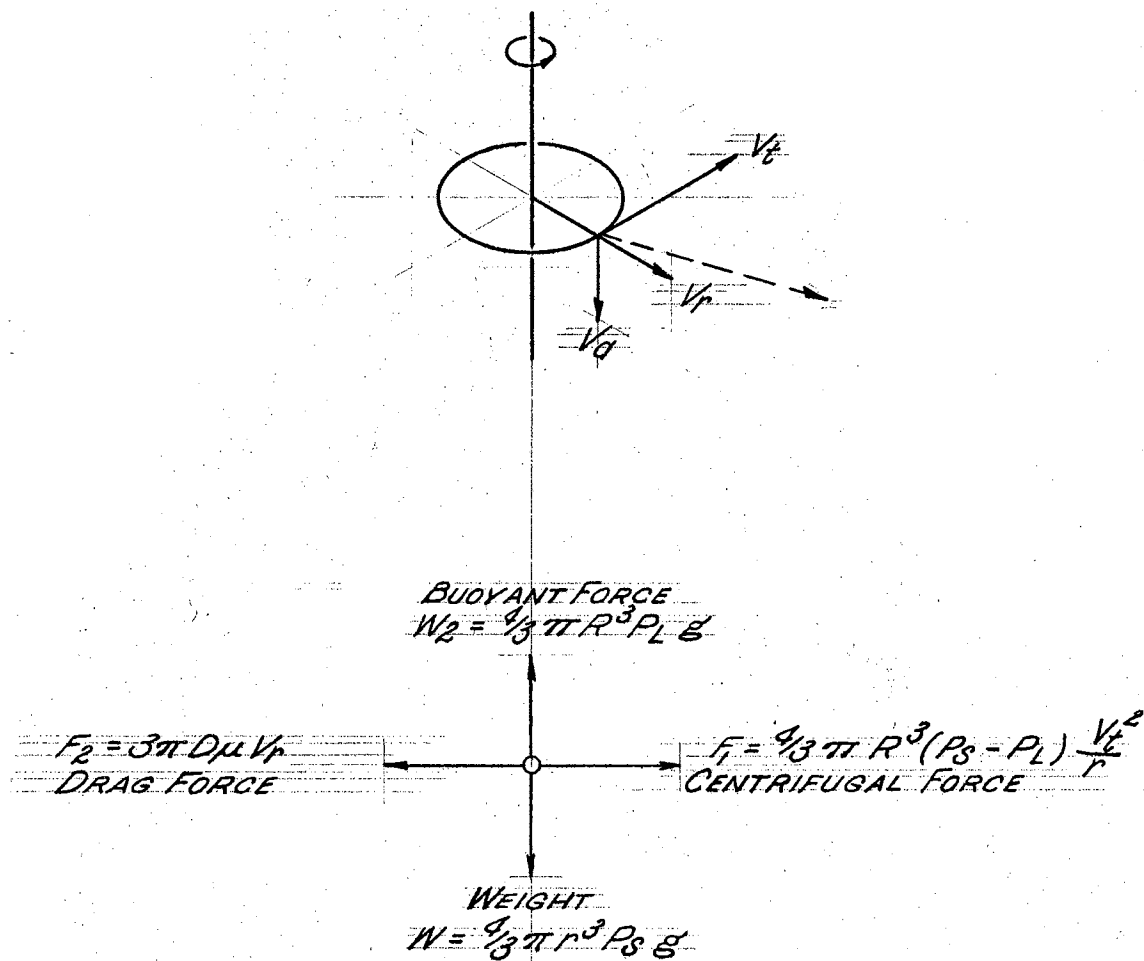


Figure 5. Forces Acting on Spherical Particle

The drag force is given by Stokes' Law for viscous flow. For flow around a sphere, the shear drag is  $2/3$  and the pressure drag is  $1/3$  of the total drag. From Albertson, et al. (10), it was shown that from the theory of Stokes for flow around a sphere, the expression for the drag force is the product of the surface area of the sphere and the unit total drag.

$$F_D = (\pi D^2)(3\mu V_o/D) . \quad (4-4)$$

The above authors have shown that the drag force can be solved by dimensional analysis to give the general drag equation,

$$F_D = C_D A \rho V_o^2 / 2 . \quad (4-5)$$

Experimental data has shown that for laminar flow, ( $Re < 0.5$ ),  $C_D$  is equal to  $24/Re$  for a sphere. This expression for the coefficient of drag and the general drag equation (4-5) combine to give Stokes' Law for viscous flow around a sphere as follows:

since

$$F_D = \frac{24}{Re} A \rho \frac{V_o^2}{2} \quad (4-6)$$

and

$$Re = \frac{V_o D}{\nu}, \quad A = \frac{\pi D^2}{4}, \quad \mu = \nu \rho \quad (4-7)$$

the drag force is

$$F_D = 3\mu\pi DV_0 \quad (4-8)$$

Substituting expressions (4-2), (4-3), and (4-8) into expression (4-1) produces the differential equation of spherical particle movement in a hydroclone,

$$\frac{4}{3}\pi R^3 \rho_s \frac{dV_r}{dt} = \frac{4}{3}\pi R^3 (\rho_s - \rho_L) \frac{V_t^2}{r} - 3\mu\pi DV_0 \quad (4-9)$$

The term,  $V_0$ , is the velocity of flow past the sphere relative to the fluid. The velocity term will be derived with the assumption that all fluid will pass through the overflow nozzle and no fluid will report to the underflow pot. For a hydroclone with an underflow pot, this assumption should not deviate enough to affect the results obtained experimentally. Because the fluid is removed through the overflow nozzle, a centripetal or negative flow will result with a velocity that will be designated as  $U_1$ . Therefore, the term,  $V_0$ , will be given by

$$V_0 = V_r - U_1 \quad (4-10)$$

where  $U_1$  is the centripetal or negative velocity of the fluid and  $V_r$  is the radial velocity of the sphere. The centripetal flow will be derived as flowing through coaxial cylinders with unit height and will be equal to the flow constant,  $Q_c$ , thus

$$Q_c = -U_1(2\pi r)(\text{unit height}). \quad (4-11)$$

The flow constant will be equal to the product of the velocity of the fluid passing through the outer area of the inner vortex and the unit height of the hydroclone section and is equal to

$$Q_c = V_{iv}(2\pi r_{iv})l. \quad (4-12)$$

The outer area of the inner vortex is equal to the product of the circumference and the length of the inner vortex and is as follows:

$$A_{iv} = 2\pi r_{iv} \left( \frac{r_c}{\tan \frac{\phi}{2}} \right) \quad (4-13)$$

The velocity of the fluid passing through the outer area of the inner vortex is equal to the inlet flow rate  $Q$  divided by the area of the inner vortex or

$$V_{iv} = \frac{Q}{A_{iv}} = \frac{Q}{(2\pi r_{iv}) \left( \frac{r_c}{\tan \frac{\phi}{2}} \right)} \quad (4-14)$$

and

$$Q_c = V_{iv}(2\pi r_{iv}) = \frac{Q}{(2\pi r_{iv}) \left( \frac{r_c}{\tan \frac{\phi}{2}} \right)} (2\pi r_{iv})$$

or

$$Q_c = \frac{Q \tan \frac{\phi}{2}}{r_c}. \quad (4-15)$$

Therefore, the centripetal or negative velocity term,  $U_1$ , will be given by

$$U_1 = - \frac{Q_c}{2\pi r} \quad (4-16)$$

or

$$U_1 = - \frac{Q \tan \frac{\phi}{2}}{2\pi r r_c} \quad (4-17)$$

The algebraic sum of  $U_1$  and  $V_r$  will be equal to  $V_o$  and is as follows:

$$V_o = V_r - U_1 = V_r + \frac{Q \tan \frac{\phi}{2}}{2\pi r r_c} \quad (4-18)$$

Substituting expression (4-18) into the differential equation (4-9), the general differential equation for a spherical particle in a hydroclone is

$$\rho_s \frac{4}{3}\pi R^3 \frac{dV_r}{dt} = \frac{4}{3}\pi R^3 (\rho_s - \rho_L) \frac{V_t^2}{r} - 6\pi R\mu \frac{dr}{dt} + \left[ \frac{Q \tan \frac{\phi}{2}}{2\pi r r_c} \right] \quad (4-19)$$

The tangential velocity can be expressed by

$$r^n V_t = k'' \quad (4-20)$$

and the constant,  $k''$ , can be evaluated by the boundary condition of  $V_t = V_i$  when  $r = r_c$ , yielding

$$V_i r_c^n = k'' \quad (4-21)$$

Since the tangential velocity at the inlet,  $V_i$ , can be calculated by dividing the flow rate by the inlet area, it

is possible to evaluate the tangential velocity field as follows:

$$V_t r^n = V_i r_c^n \quad (4-22)$$

$$V_i = \frac{Q}{A_i} = \frac{Q}{\pi r_i^2} \quad (4-23)$$

Therefore, 
$$V_t = \frac{Q}{\pi r_i^2} \left( \frac{r_c}{r} \right)^n \quad (4-24)$$

and 
$$\frac{V_t^2}{r} = \frac{\frac{Q^2}{\pi^2 r_i^4} \left( \frac{r_c}{r} \right)^{2n}}{r} \quad (4-25)$$

yielding the differential equation

$$\frac{dV_r}{dt} = \left( \frac{\rho_s - \rho_L}{\rho_s} \right) \frac{\frac{Q^2}{\pi^2 r_i^4} \left( \frac{r_c}{r} \right)^{2n}}{r} - \frac{18\mu}{\rho_s} \frac{1}{D^2} \frac{dr}{dt} - \frac{Q \tan \frac{\phi}{2} 18\mu}{\rho_s 2\pi r r_c D^2} \quad (4-26)$$

This is the differential equation that will be solved on the analog computer. The following expressions, based on the literature survey and practical considerations, are substituted into expression (4-26):

$$4r_i = r_c$$

$$n = 0.5$$

$$\phi = 10 \text{ degrees}$$

$$\mu = \text{MIL} - 0 - 5606 @ 80^\circ\text{F} = 2.48 \times 10^{-6} \frac{\text{lb. sec.}}{\text{in.}^2}$$

$$Q_{15}^2 = 3330 \text{ in.}^6/\text{sec.}^2$$

$$Q_{15} = 57.7 \text{ in.}^3/\text{sec.}$$

$$D_{10}^2 = 15.45 \times 10^{-8} \text{ in.}^2$$

$$r_{0.25}^3 = 1.56 \times 10^{-2} \text{ in.}^3$$

$$r_{0.25} = 2.5 \times 10^{-1} \text{ in.}$$

$$\rho_S = 0.0904 \text{ lb./in.}^3$$

$$\rho_L = 0.0309 \text{ lb./in.}^3 \quad .$$

Substituting into equation (4-26), the first term is equal to

$$3.66 \times 10^6 \left( \frac{Q}{Q_{15}} \right)^2 \left( \frac{r_{0.25}}{r} \right)^3 \frac{1}{r^2} ,$$

the second term

$$1.235 \times 10^6 \left( \frac{D_{10}}{D} \right)^2 \frac{dr}{dt} ,$$

and the last term is

$$\frac{3.98 \times 10^6}{r} \left( \frac{Q}{Q_{15}} \right) \left( \frac{r_{0.25}}{r} \right) \left( \frac{D_{10}}{D} \right)^2$$

Combining these terms and letting

$$\left( \frac{Q}{Q_{15}} \right)^2 \left( \frac{r_{0.25}}{r} \right)^3 = A \quad (4-27)$$

$$\left( \frac{D_{10}}{D} \right)^2 = B \quad (4-28)$$

and

$$\left( \frac{Q}{Q_{15}} \right) \left( \frac{r_{0.25}}{r} \right) \left( \frac{D_{10}}{D} \right)^2 = C , \quad (4-29)$$



the differential equation in terms of the three parameters A, B, and C is

$$\frac{dV_r}{dt} = A3.66 \times 10^6 \frac{1}{r^2} - B1.235 \times 10^6 \frac{dr}{dt} - C \frac{3.98 \times 10^6}{r} \quad (4-30)$$

where r is in inches and t in seconds. After scaling for the analog computer (Appendix A), the equation is

$$\frac{dV_r}{dt} = A3.66f(r) - B1.235 \times 10^2 \frac{dr}{dt} - C \frac{3.98 \times 10^2}{r} \quad (4-31)$$

where

$$f(r) = \frac{10^4}{r^2} \quad (4-32)$$

and r is in volts and t in centiseconds.

The values that were used for the plot of flow rate versus hydroclone radius (Figure 6), were read directly from the analog computer and do not represent the maximum radius that the particle would attain while in the hydroclone. The values of flow rate and  $r_c$  selected for the plot were those for which  $r(t)$  (radius a particle is at time t) increased from a previous negative or zero reading. A minimum time was selected for each hydroclone radius, and the voltmeter reading or  $r(t)$  was recorded for the different flow rates and particle diameters. A longer time, below the maximum time in the hydroclone, was allowed for

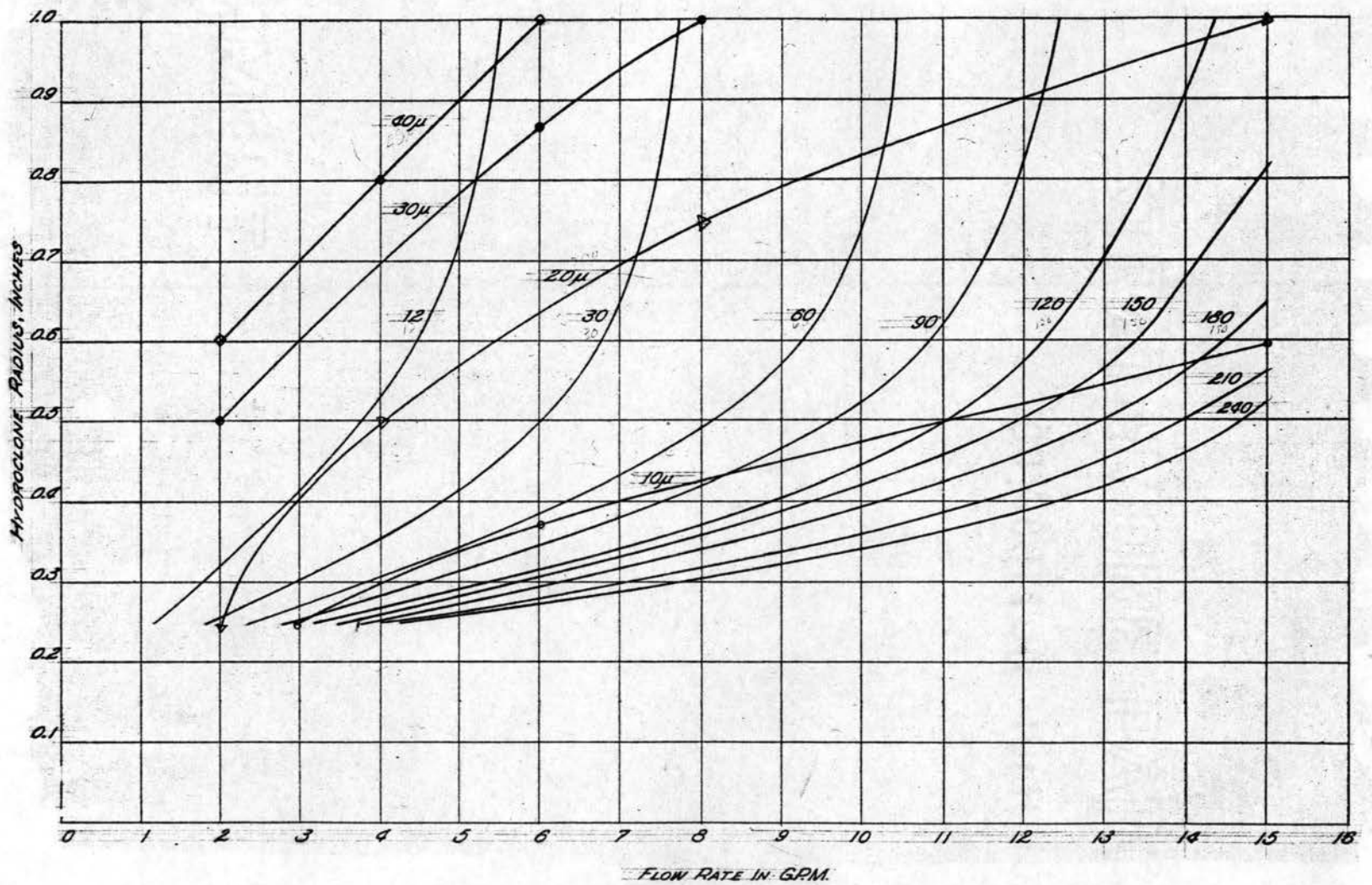


Figure 6. Hydroclone Radius Versus Flow Rate Plot

values that were near zero to determine whether  $r(t)$  was increasing or decreasing with respect to time. However, the values of zero reading, or the equilibrium radius, could be used if the particle could be placed at the outer wall when entering the hydroclone.

The plot is limited from 2 to 15 gpm and 0.25 to 1.00 inch radius hydroclone with particles ranging from 10 to 40 microns in increments of 10 microns.

A specific micron size can be removed if the intersection of the flow rate and hydroclone radius are below the specific micron curve. For example, a minimum of 3 gpm with a hydroclone radius of 0.25 inches is required for removal of a 10 micron particle and a value of 6 gpm or greater and a hydroclone radius of 1.00 inches or smaller will remove a 40 micron particle.

Experimental data was used to superimpose curves of constant pressure drop on the plot shown in Figure 6,  
page 28.

TABLE I  
PARTICLE RADIUS

Particle Diameter (Microns)			10	20	30	40
Flow Rate (GPM)	15 *	$r_c = 0.25$ inches	1.2	4.1	7.0	10.9
	12		1.0	3.0	5.5	8.2
	10		0.9	2.8	4.4	6.3
	8		0.8	1.2	2.8	4.0
	5		0.3	0.8	1.5	2.0
	4		0.1	-	-	-
	3		0.1	-	-	-
	2		0	0.1	0.2	1.0
	6	$r_c = 0.37$ inches	0.1	-	-	-
	15		1.0	3.2	5.5	9.5
	12		0.4	2.0	4.5	7.0
	10		0.2	1.8	3.5	5.5
	8		0.1	1.0	2.4	3.4
	5		0	0.3	1.0	1.8
	4		-	0.1	-	-
	2		0	0	0.1	0.2
	15	$r_c = 0.50$ inches	0.1	-	-	-
	2		-	-	-	0.1
	15		-0.1	1.3	3.2	5.8
	12		-0.2	0.9	2.2	4.1
	10		-0.1	0.5	1.5	2.9
	8		-0.2	0.2	1.1	1.8
	6		-	-	0.1	-
	5		-0.1	0	0	0.9
	4		-	-	-	0.1
	2		0	0	0	0
	4	$r_c = 0.60$ inches	-	-	-	0.1
	6		-	-	0.1	-
	15		-0.8	0.1	1.4	2.8
	12		-0.5	0	1.0	2.0
	10		-0.4	0	0.6	1.3
	9		-	-	0.3	-
	8		-0.3	-0.1	0.1	0.6
	6		-	-	-	0.5
	5		-0.2	-0.1	-0.1	0
	2		-0.1	-0.1	-0.1	-0.2
	4	$r_c = 0.75$ inches	-	-	-	0.1
	6		-	-	0.1	-
	15		-0.8	0.1	1.4	2.8
	12		-0.5	0	1.0	2.0
	10		-0.4	0	0.6	1.3
	9		-	-	0.3	-
	8		-0.3	-0.1	0.1	0.6
	6		-	-	-	0.5
	5		-0.2	-0.1	-0.1	0
	2		-0.1	-0.1	-0.1	-0.2
	4	$r_c = 0.80$ inches	-	-	-	0.1
	6		-	-	0.1	-
	15		-0.8	0.1	1.4	2.8
	12		-0.5	0	1.0	2.0
	10		-0.4	0	0.6	1.3
	9		-	-	0.3	-
	8		-0.3	-0.1	0.1	0.6
	6		-	-	-	0.5
	5		-0.2	-0.1	-0.1	0
	2		-0.1	-0.1	-0.1	-0.2
	4	$r_c = 0.87$ inches	-	-	-	0.1
	6		-	-	0.1	-
	15		-0.8	0.1	1.4	2.8
	12		-0.5	0	1.0	2.0
	10		-0.4	0	0.6	1.3
	9		-	-	0.3	-
	8		-0.3	-0.1	0.1	0.6
	6		-	-	-	0.5
	5		-0.2	-0.1	-0.1	0
	2		-0.1	-0.1	-0.1	-0.2
	4	$r_c = 1.00$ inches	-	-	-	0.1
	6		-	-	0.1	-
	15		-0.8	0.1	1.4	2.8
	12		-0.5	0	1.0	2.0
	10		-0.4	0	0.6	1.3
	9		-	-	0.3	-
	8		-0.3	-0.1	0.1	0.6
	6		-	-	-	0.5
	5		-0.2	-0.1	-0.1	0
	2		-0.1	-0.1	-0.1	-0.2

\*Note: Values in Table I are inches  $\times 10^2$ .

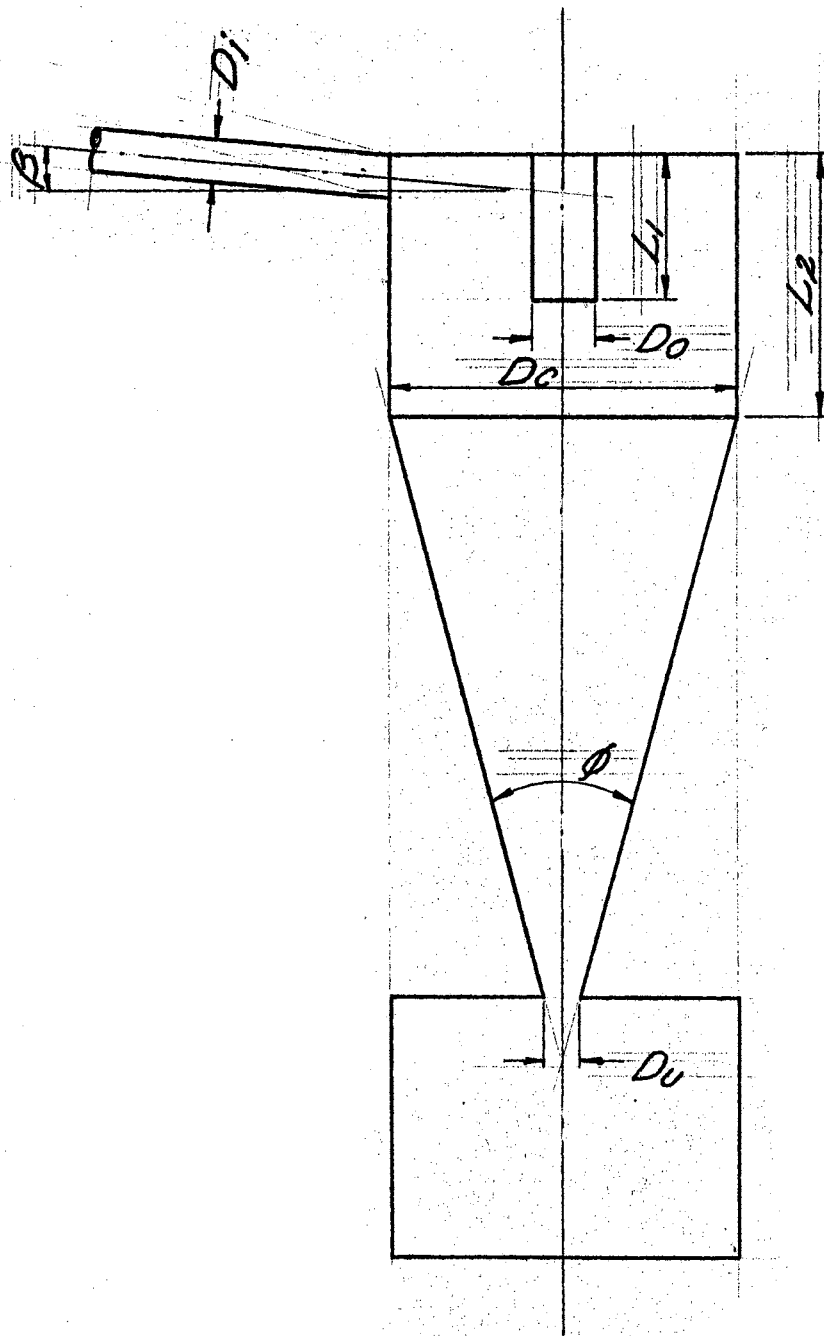


## CHAPTER V

### EXPERIMENTAL VERIFICATION

Hydroclones of 0.281, 0.500, and 1.00 inch radii were built to test the validity of the results obtained from the solution of the analytical expression. The hydroclones that were built had several dimensions fixed because of the relationships used in the derivation of the analytical expression. The inlet nozzle radius be equal to one-fourth of the hydroclone radius. A 10 degree included cone angle was used for all hydroclones. The length of the cylindrical section,  $l$ , was equal to the diameter of the hydroclone (Figure 7). The same underflow pot was used for all hydroclone tests. The overflow nozzle radius was equal to the radius of the inlet nozzle and the underflow radius was equal to one-eighth of the hydroclone radius. The underflow diameter was established by trying several cones of different size and selecting the one that gave the best separation efficiency. A table of the above dimensions are shown in Figure 7 for the different hydroclones.

The conical section of the hydroclones were made by pouring epoxy resin around an aluminum mandrel and then machined to fit in the center section of the hydroclone.



$D_c$	$D_i$	$D_o$	$D_u$	$L_2$	$L_1$
0.562	0.1405	0.1405	0.0707	0.562	0.281
1.000	0.2500	0.250	0.1250	1.000	0.500
2.000	0.500	0.500	0.2500	2.000	1.000

$\beta = 5$  degrees

Figure 7. Hydroclone Dimensions

This type of fabrication provided a smooth cone which helped decrease pressure drop and cost (Figure 8). An electrical and pilot operated power stand built by Oklahoma State University to conduct filter studies for Tinker Air Force Base was used for testing the hydroclones (Figures 9, 10, 11). A measured amount of hydraulic fluid and contaminant was injected for each flow rate. The contaminant was fine AC test dust that has a density relatively close to that of glass beads. This contaminant was used because glass beads tended to choke the automatic particle counter. A malt mixer was used to prepare the contaminant that was poured into the injection cylinder. Equal volumes of sample fluid were taken in equal periods of time to determine the per cent of separation efficiency. The flow rate was also recorded during injection because of an increase in total flow due to the injection cylinder. The sample valves were allowed to bleed before the fluid samples were taken to make certain that particles trapped in the various fittings would not become dislodged during injection and give an erroneous result. Sample bottles were rinsed with a filtered solvent to reduce background particles in the fluid. The samples taken were evaluated immediately so that they would not be given a chance to be self-contaminated by the bottles.

Beginning with a maximum of 15 gpm, the flow rate was decreased in increments of approximately 1 gpm and samples were taken before and after the hydroclone. Temperature

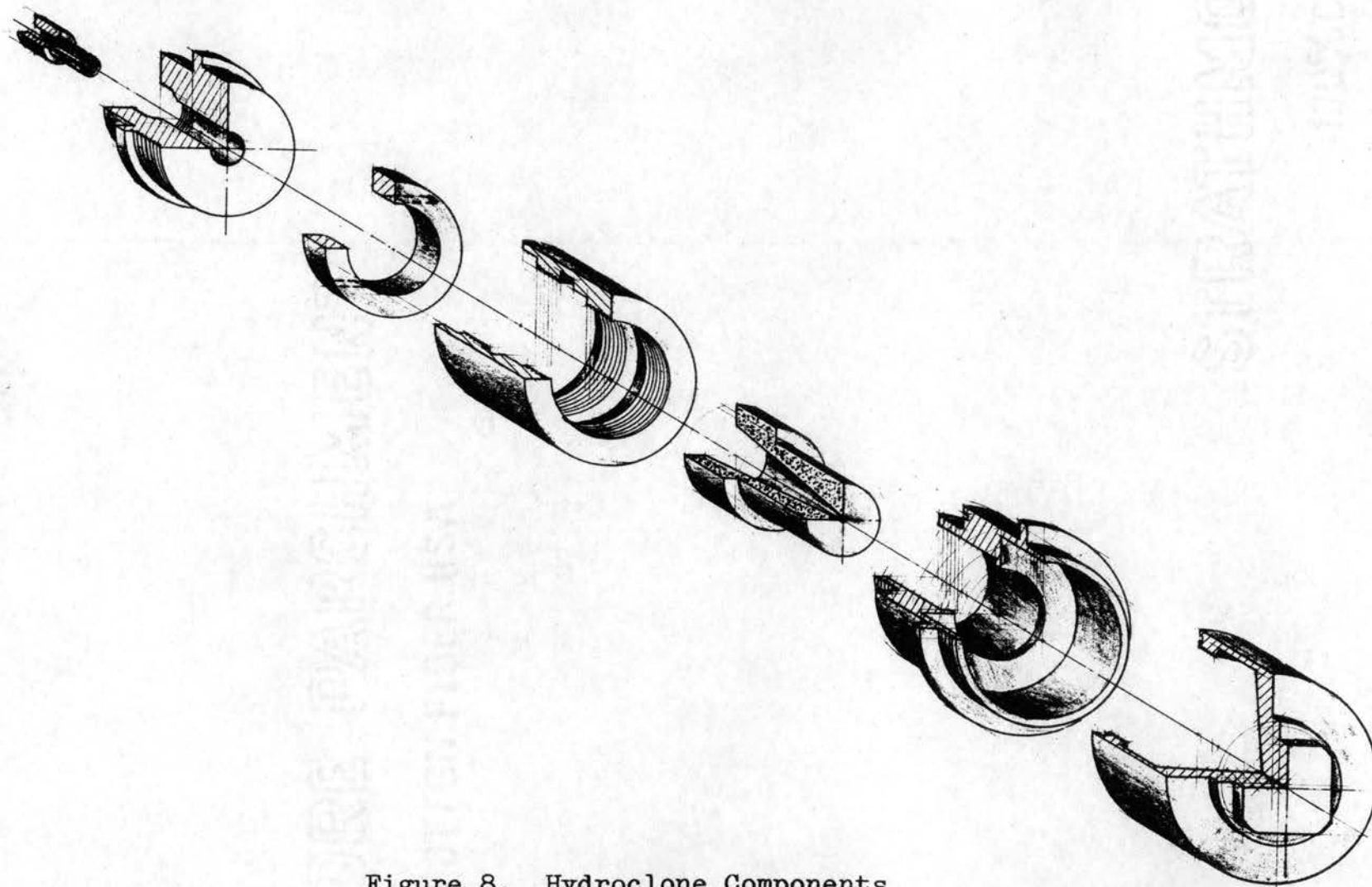


Figure 8. Hydroclone Components



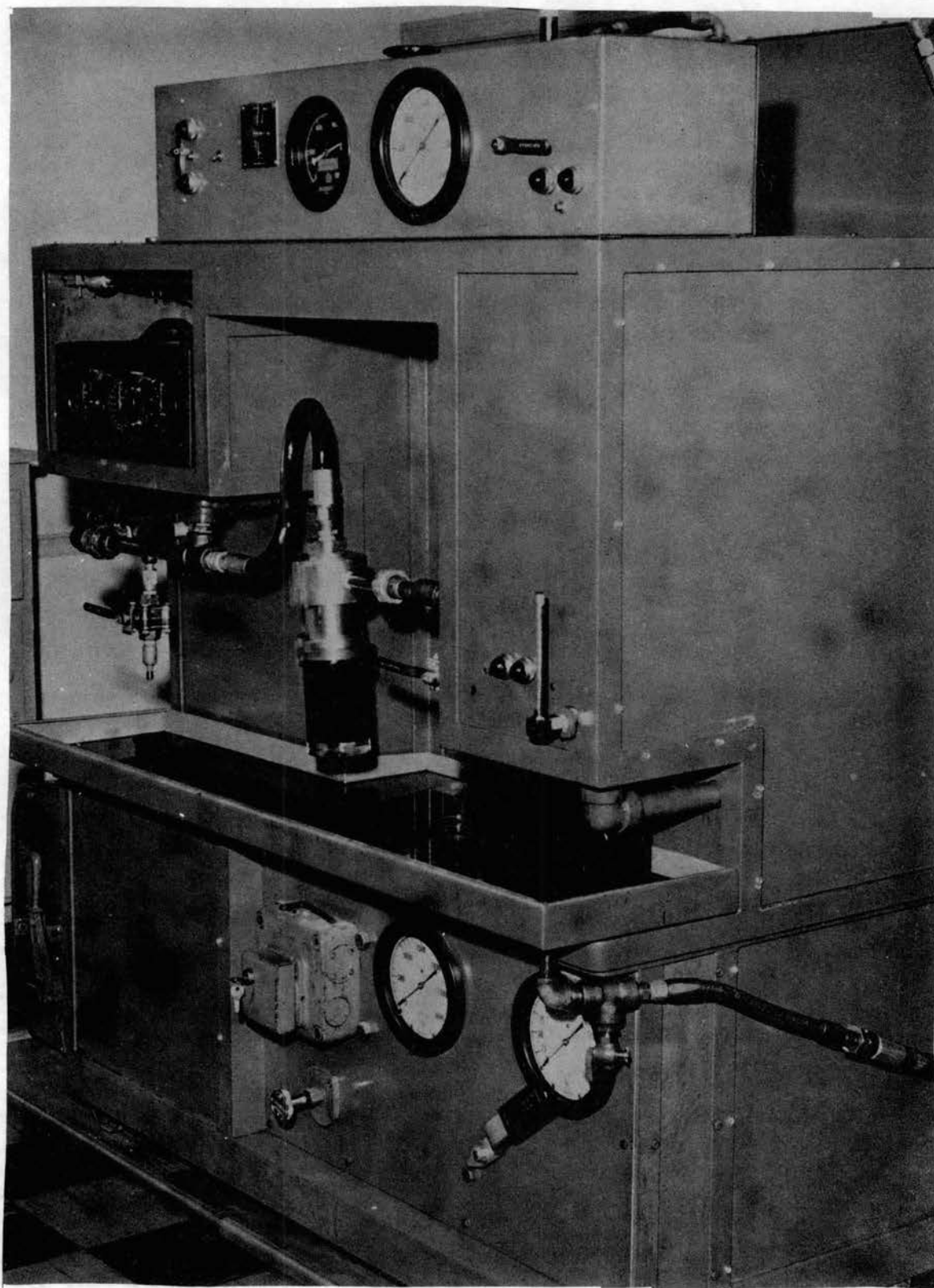


Figure 9. Power Stand

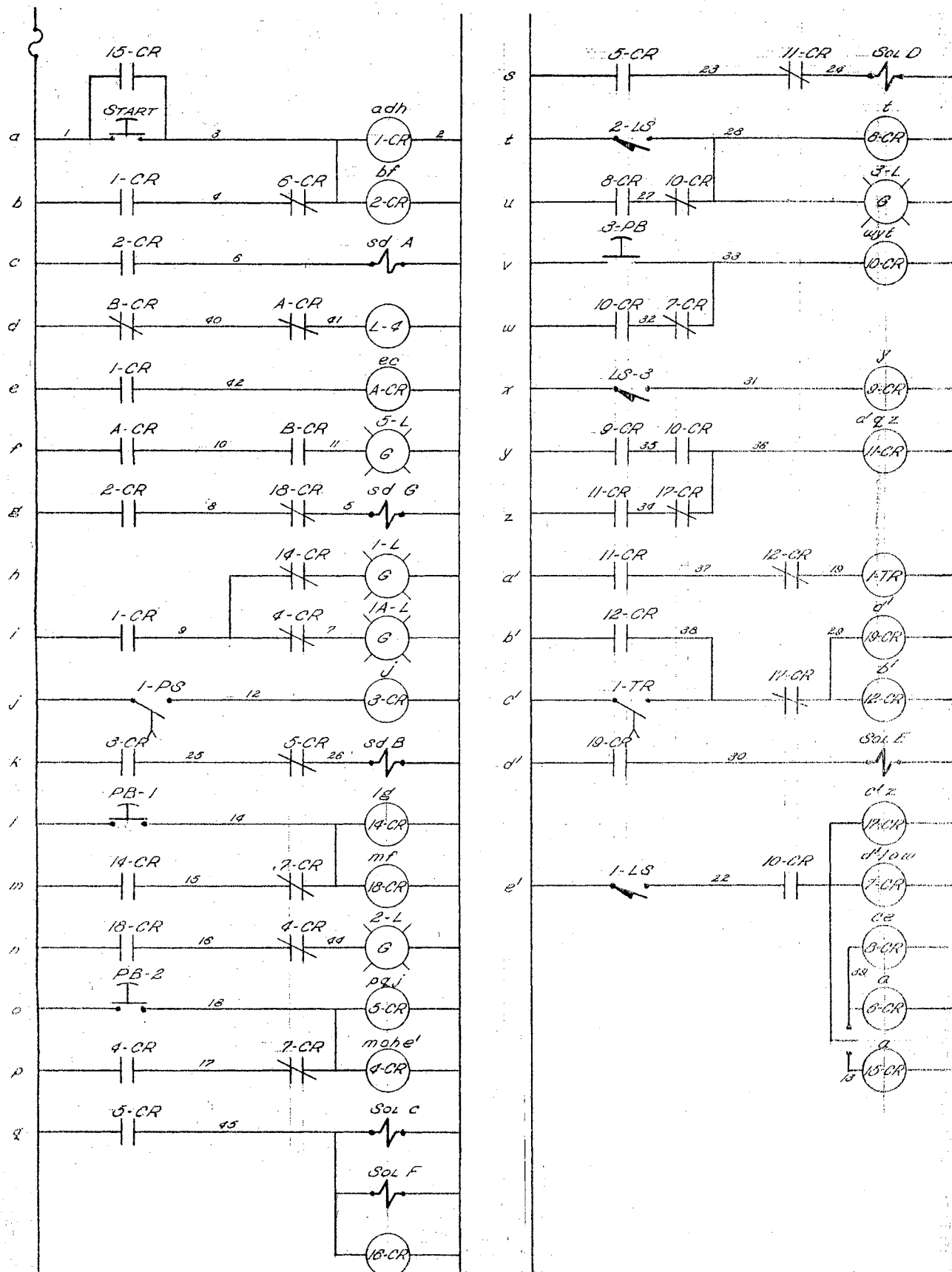


Figure 10. Electrical Schematic for Power Stand

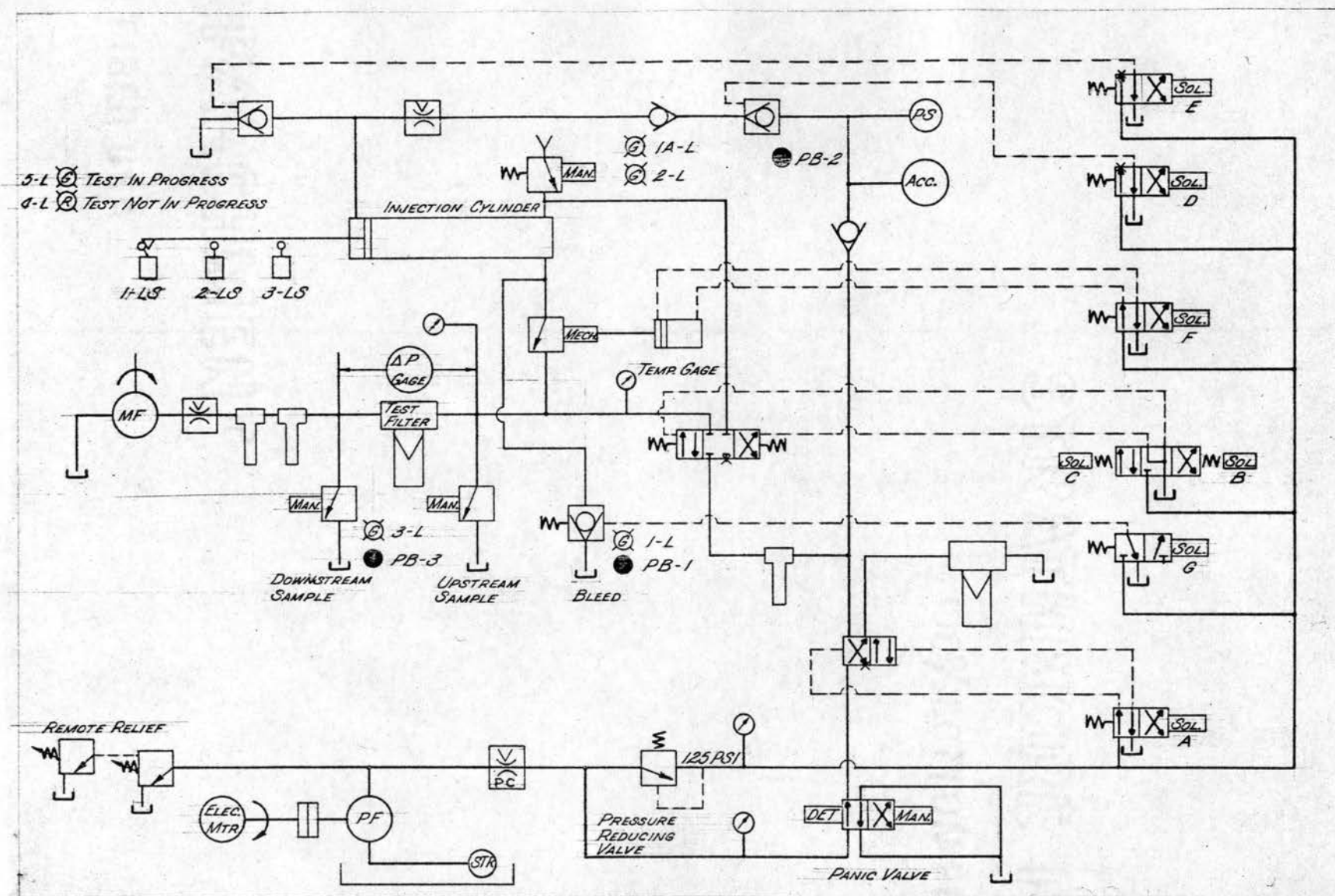


Figure 11. Hydraulic Schematic for Power Stand

remained constant between 85 and 90 degrees Fahrenheit, depending on the particular hydroclone. As the hydroclone diameter was reduced, the pressure drop increased which resulted in a higher constant temperature system.

An electronic particle counter, described in detail in Appendix C, was used to determine the percentage of contaminant removed by the different hydroclones. The particle counter records all particles that are equal to or greater than the size set on the threshold dial. The number of particles in a particular size range can be determined by subtracting both the particles above the range and the background particles that are present in the rinsing solvent and electrolyte. For example, all the particles between 10 and 11 microns can be found by taking the number of 11 micron particles and subtracting the number of 10 micron and background particles.

Several samples were taken at the flow rates where the separation efficiency apparently was incorrect in order to determine an average separation efficiency. Three different counts were recorded from the particle counter to obtain an average reading for the separation efficiency. Plots of separation efficiency versus flow rates for hydroclone radii of 0.281 and 0.500 inches are shown in Figures 12 and 13 respectively.

The plot of hydroclone efficiency versus flow rate for the 0.500 inch radius hydroclone in Figure 12 indicates that the curves obtained from the analog computer

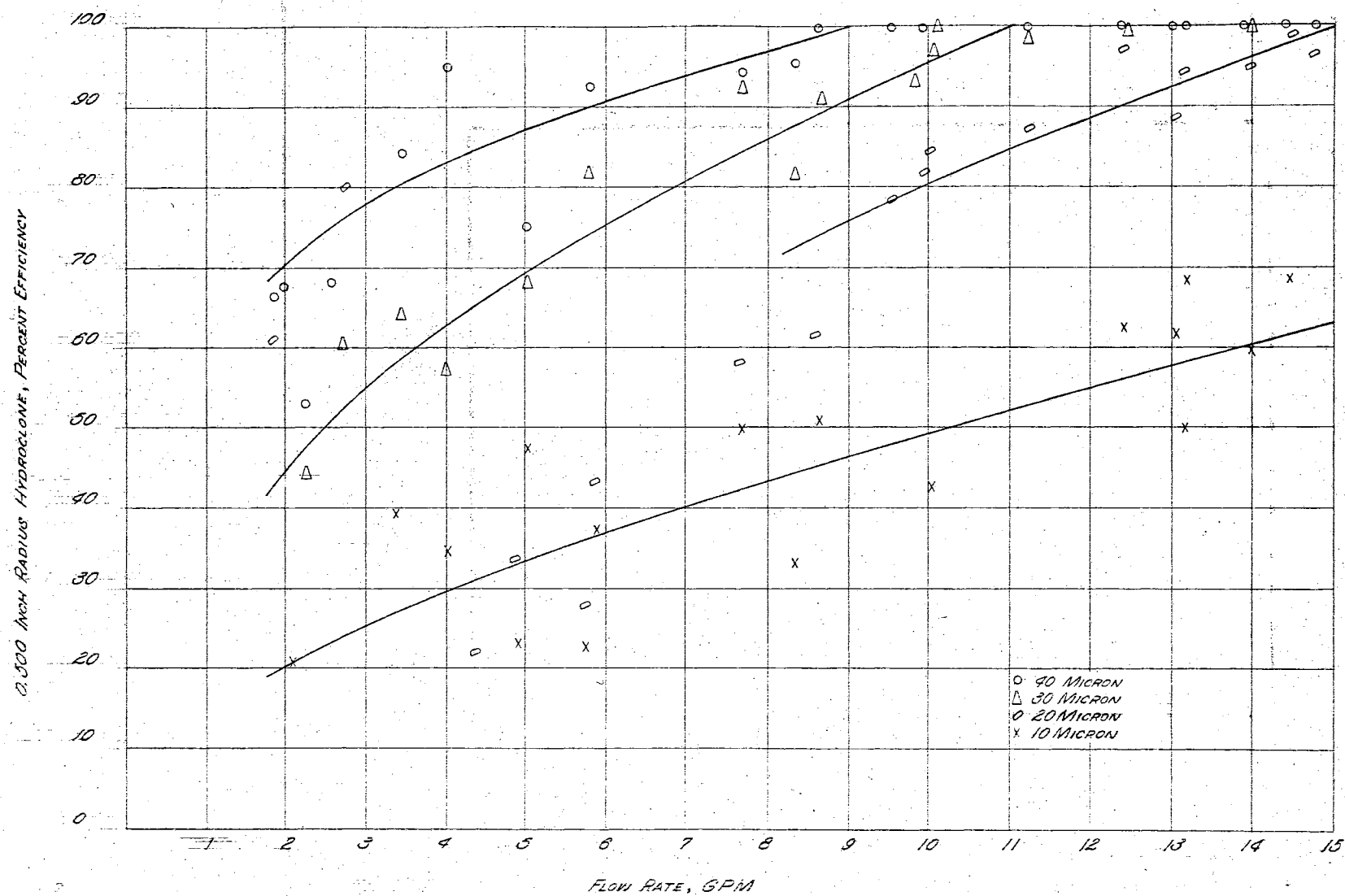


Figure 12. 0.500 Inch Radius Hydroclone Separation Efficiency Plots

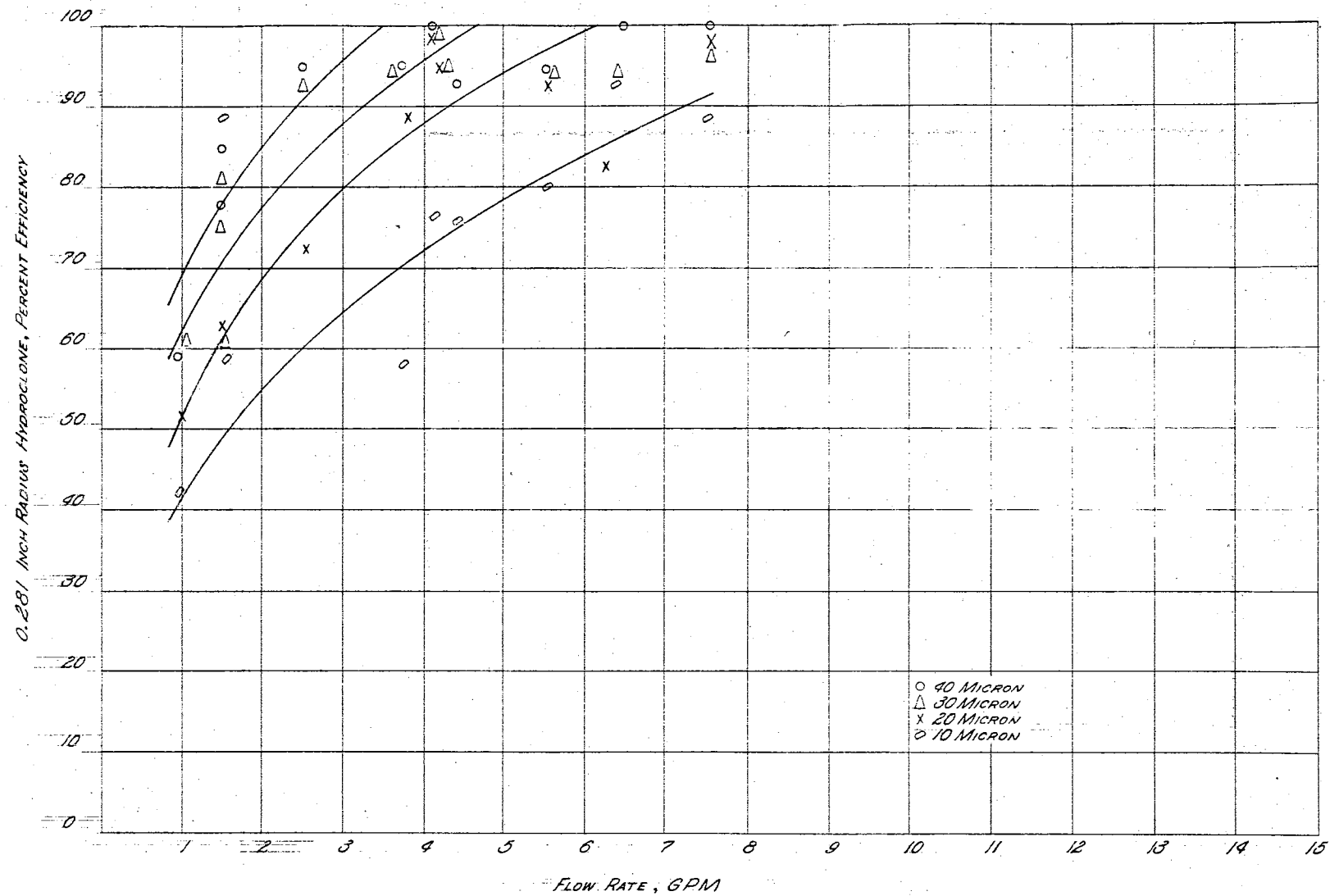


Figure 13. 0.281 Inch Radius Hydroclone Separation Efficiency Plots



represent the point at which 50 per cent of the contaminant is removed from the fluid. Flow rate values of 50 per cent efficiency from Figure 12 (page 39) are superimposed on the results of the analog computer in Figure 14. The reason that the lines represent 50 per cent elimination can be explained by the fact that the values plotted from the analog computer were taken where the radius was increasing slightly with respect to time or near the equilibrium point. The particles may report to the overflow nozzle or to the underflow pot as a result of being near this equilibrium point.

The points for 10, 30, and 40 microns for the 0.500 inch radius hydroclone follow an expected pattern. However, the points for the 20 micron line were unstable below 8 gpm and the values for flow rates below 6 gpm for all curves were to some extent unstable. At the smaller flow rates, it is possible that a strong vortex pattern may not be well established and secondary flows may interfere with the vortex flows which are necessary for hydroclone operation.

The maximum flow rate that the power stand could provide was not sufficient to test the 1.00 inch radius hydroclone. Here again, the influence of secondary flows over the vortex flows tend to make the results inconsistent. A flow rate of 25 gpm or greater would be necessary to evaluate the 1.00 inch radius hydroclone to obtain a set of good curves for the different micron sizes.

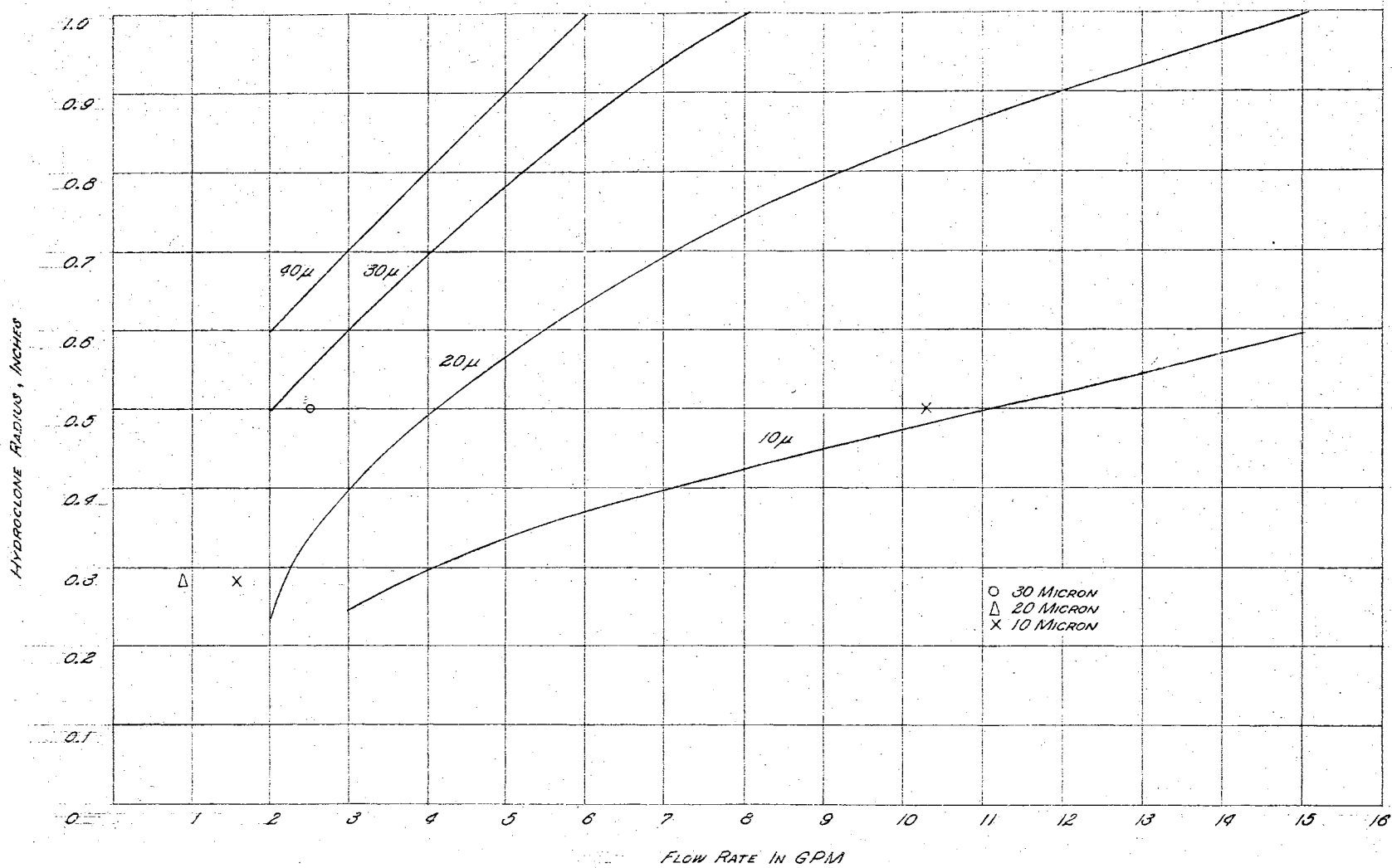


Figure 14. Comparison of Experimental and Analog Computer Results



With the power stand that was available for the testing of the 0.281 inch radius hydroclone, a maximum flow rate of 7 gpm was obtained. The differential pressure gauge that was available has a maximum range of 300 psi and, therefore, the pressure drop across the hydroclone could not be recorded for this flow rate. However, the pressure drop was near 700 psi or the setting on the relief valve and this governed the flow rate.

The experimental results for the 0.281 inch radius hydroclone, shown in Figure 13 (page 40), were more consistent than the larger hydroclones. This also may be a result of a stronger vortex generated because of the small hydroclone radius and the relative larger flow rates. The value from the experimental results for the flow rate necessary for 50 per cent separation efficiency at 20 microns for the 0.281 inch radius hydroclone was 0.9 gpm as compared to 2.3 gpm predicted by the analog computer.

## CHAPTER VI

### CONCLUSIONS

The results from the analog computer and experimental tests show that the analytical expression (4-26) can be used to predict the movement of a particle in a hydroclone. A plot of the 50 per cent separation efficiency curves can be obtained by using the values from the analog computer where the radius of the particle increased from a previous zero or negative reading to a positive reading as a result of increasing the flow rate.

The analytical expression (4-26) was derived on the assumption that secondary flows do not exist and a particle can be removed if the centrifugal force is greater than the drag force and sufficient time is permitted for the particle to move to the outer wall and be discharged into the underflow pot. Flow rates below 6 gpm gave results that were unstable for a 0.500 inch radius hydroclone and may be caused by secondary flows that interfere with vortex flows which are necessary for hydroclone operation.

Because of secondary flows which decrease separation efficiency, the flow rate must be increased as the hydroclone radius increases in order to generate a strong vortex which is necessary for hydroclone operation.

Therefore, a flow rate of 25 gpm or greater would be necessary to evaluate a hydroclone of 1.00 inch radius in the range from 10 to 40 microns.

It was further evidenced that the 0.281 inch radius hydroclone gave consistent results until the flow rate was decreased to 0.5 gpm.

It is the opinion of the author that a hydroclone in series with a filter could be used in a system where absolute cleanliness is demanded to considerably increase the life of the filter and reduce the cost of cleaning or replacing the filter element. It is also evident that the size of a hydroclone is usually smaller when compared to a filter for the same flow rate. This study indicates that a hydroclone also provides a sharper classification in micron particle separation than a conventional filter element.

Based on the fine correlation between the analytical and experimental results, it is concluded that a hydroclone can be built to perform a predicted operation.

## CHAPTER VII

### RECOMMENDATIONS FOR FUTURE STUDY

Expression (4-26) is the general differential equation of a particle in a hydroclone and was used to predict the effects of changing the hydroclone radius, flow rate, and particle size. However, this equation could be used to show the effects of increasing or decreasing the temperature of the fluid, the angle of the cone, and the density of other particles.

The underflow pot could be a source of inefficiency and should be investigated to reveal existing flow patterns which might pick up particles in the pot and return them to the overflow nozzle.

A contour head could be designed that might help to eliminate short circuit flow patterns occurring at the tip of the vortex finder.

#### A SELECTED BIBLIOGRAPHY

1. Matschke and Dahlstrom, D. A. Chemical Engineering Progress, Vol. 34, No. 12, (December, 1958 and January, 1959).
2. Haas, Nurmi, Whatley, and Engle. Chemical Engineering Progress, Vol. 53, No. 4, Page 205 (April, 1957).
3. Dahlstrom, D. A. Mining Transactions, Vol. 184, (September, 1949).
4. Yoshioka, N., and Hotta. Chemical Engineering (Japan) Page 632-640 (1955).
5. Moder, J. J. Ph.D. Thesis, Northwestern University (1950).
6. Driessen, M. G. Rev. Ind. Minerale, Page 449 (March 31, 1951).
7. Kelsall, D. F. Chemical Engineering Science, Vol. 2, Page 266, (1953).
8. Criner, H. E. Paper presented at International Conference on Coal Preparation, Paris (1950).
9. Shepherd and Lapple, Industrial and Engineering Chemistry, Vol. 53, No. 4, Page 205 (April, 1957).
10. Albertson, Barton, and Simons, Fluid Mechanics for Engineers, New Jersey: Prentice-Hall, Inc., Page 433, 1960.
11. Gilbert, J. S. Master's Thesis, Oklahoma State University (1960).
12. Beattie, J. F. Master's Thesis, Oklahoma State University (1961).

## APPENDIX A

The differential equation,

$$\frac{dV}{dt} = A3.66 \times 10^6 \frac{1}{r^2} - B1.235 \times 10^6 \frac{dr}{dt} - C \frac{3.98 \times 10^6}{r} \quad (4-30)$$

was scaled for the analog computer with the following substitutions:

$$1 \text{ inch} = 100 \text{ Volts}, \quad (A-1)$$

$$1 \text{ Sec. in Problem} = 1/100 \text{ Sec Computer time.} \quad (A-2)$$

The units on the first term of the equation are  $\frac{\text{in}^3}{\text{sec}^2}$ , the second term  $1/\text{sec}$ , and the third term  $\text{in}^2/\text{sec}^2$ . Substituting the expressions (A-1) and (A-2) into equation (4-30), the first term yields,

$$A3.66 \times 10^6 \frac{1}{r^2} \frac{(100)^3 \text{ Volts}^3}{\text{cs}^2 (100)^2} = A3.66 \times 10^8 \frac{1}{r^2} \frac{\text{Volts}^3}{\text{cs}^2} \quad (A-3)$$

the second term is equal to,

$$B1.235 \times 10^6 \frac{dr}{dt} \frac{1}{\text{cs} 100} = B1.235 \times 10^4 \frac{dr}{dt} \frac{1}{\text{cs}} \quad (A-4)$$

and the third term is,

$$C \frac{3.98 \times 10^6}{r} \frac{(100)^2 \text{ Volts}^2}{(100)^2 \text{ cs}^2} = C \frac{3.98 \times 10^6}{r} \left( \frac{\text{Volts}}{\text{cs}} \right)^2 \quad (A-5)$$

Combining these terms, the equation now becomes

$$\frac{dV_r}{dt} = A3.66 \times 10^8 \frac{1}{r^2} - B1.235 \times 10^4 \frac{dr}{dt} - C \frac{3.98 \times 10^6}{r} \quad (A-6)$$

where  $r$  is in volts and time is in centiseconds.

Time for the analog computer is seconds whereas, system time for equation (A-6) is centiseconds. Therefore, this equation must be time scaled before it can be solved on the computer. Let  $\tau$  be computer time and  $t$  be system time so that  $\tau = 100t$ .

Substituting for  $t$  in equation (A-6) yields

$$10^4 \frac{dV_r}{dt} = A3.66 \times 10^8 \frac{1}{r^2} - B1.235 \times 10^4 \frac{dr}{dt} 10^2 - C \frac{3.98 \times 10^6}{r}$$

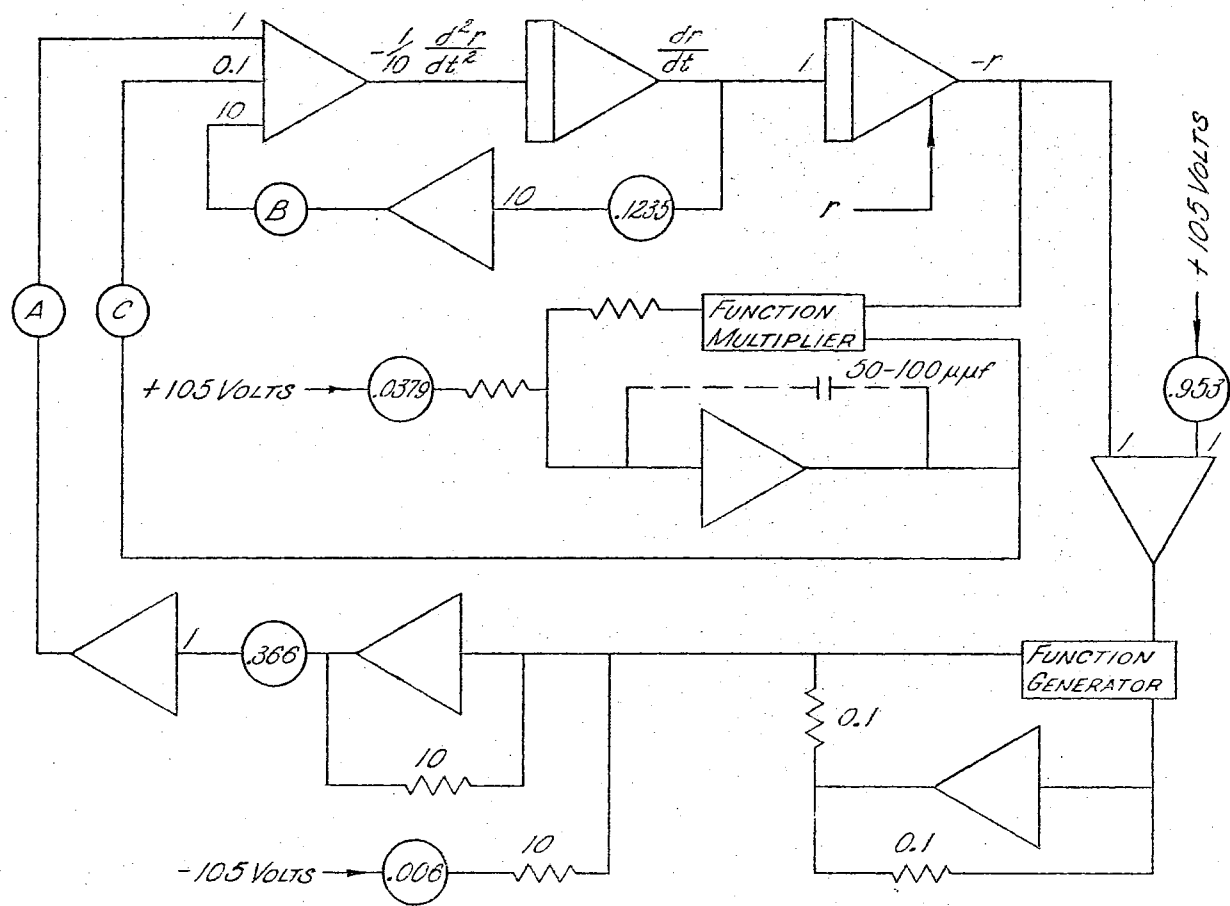
or

$$\frac{dV_r}{dt} = A3.66 \times 10^4 \frac{1}{r^2} - B1.235 \times 10^2 \frac{dr}{dt} - C \frac{3.98 \times 10^2}{r} \quad (A-7)$$

The expression  $1/r^2$  was set on the function generator of the analog computer so that  $f(r)$  will equal 100 volts when  $r$  is equal to 0.10 in. or 10 volts. Therefore,  $f(r) = 10^4/r^2$  and expression (A-7) now becomes

$$\frac{dV_r}{dt} = A3.66f(r) - B1.235 \times 10^2 \frac{dr}{dt} - C \frac{3.98 \times 10^2}{r} \quad (4-31)$$

where  $r$  is in inches and time is in centiseconds.



PROBLEM BOARD SCHEMATIC

Figure 15. Problem Board Schematic



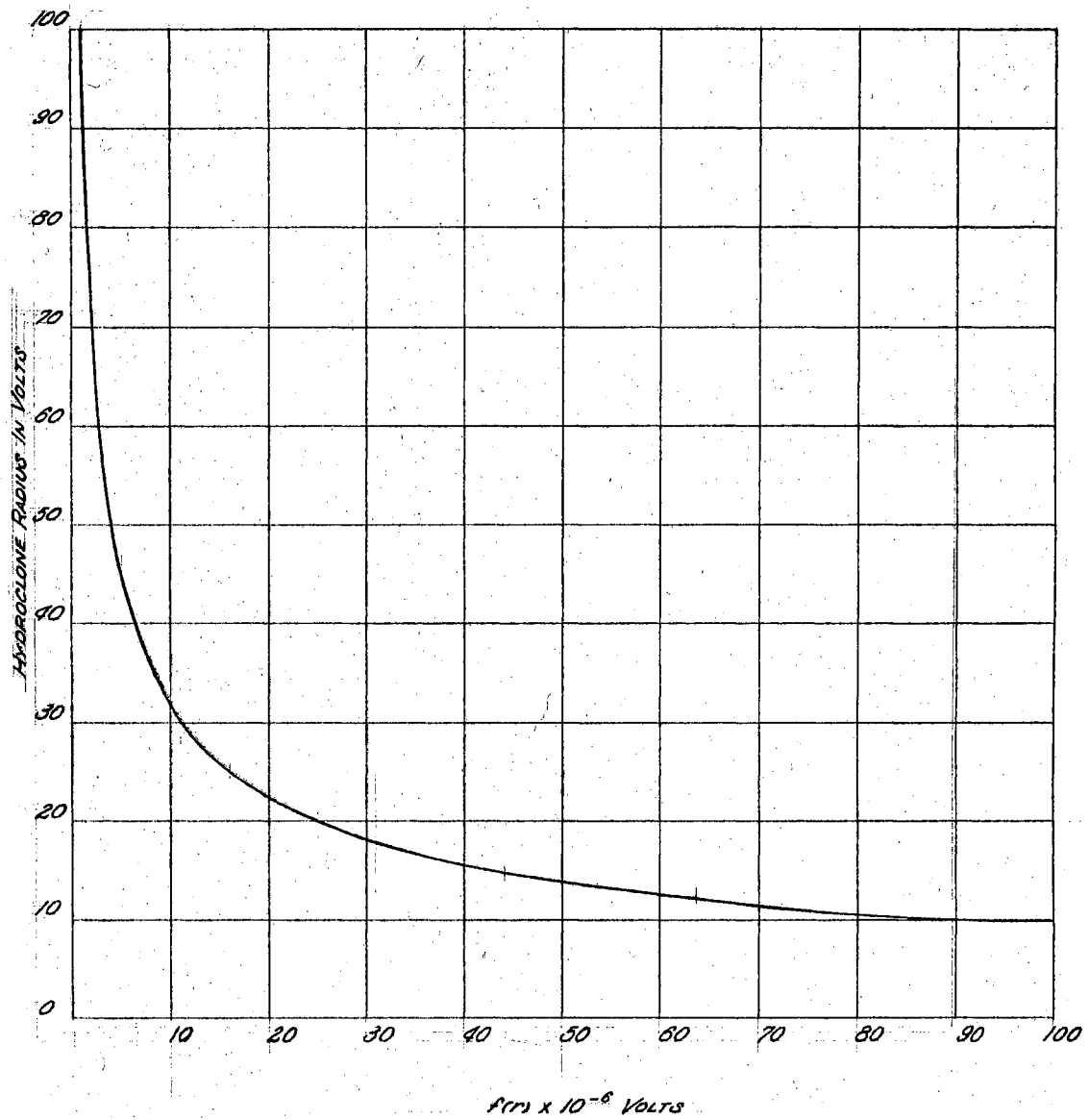


Figure 16. Function (r) Plot

TABLE II  
FUNCTION (r) DATA

$f(r) = \frac{10^4}{r^2}$			
r (inches)	r (volts)	f (r) (inches x 10 <sup>-4</sup> )	f (r) (Volts)
0	0	00	00
0.10	10	100	100
0.125	12.5	64.4	64.4
0.150	15.0	44.5	44.5
0.20	20.0	25.0	25.0
0.25	25.0	16.0	16.0
0.30	30.0	11.1	11.1
0.35	35.0	8.2	8.2
0.40	40.0	6.25	6.25
0.45	45.0	5.09	5.09
0.50	50.0	4.00	4.00
0.55	55.0	3.31	3.31
0.60	60.0	2.78	2.78
0.65	65.0		
0.70	70.0	2.04	2.04
0.75	75.0		
0.80	80.0	1.57	1.57
0.85	85.0		
0.90	90.0	1.24	1.24
0.95	95.0		
1.00	100	1.00	1.00

## APPENDIX B

### LIST OF SYMBOLS AND ABBREVIATIONS

$F_a$	Acceleration force, lb.
$F_c$	Centrifugal force, lb.
$F_d$	Drag force, lb.
$r_c$	Radius of hydroclone, in.
$r(t)$	Radius of particle at time $t$ , in.
$r_i$	Radius of inlet nozzle, in.
$r_o$	Radius of overflow nozzle, in.
$t$	Time, sec.
$L$	Length of hydroclone, in.
$R$	Radius of particle, in.
$d_{50}$	Diameter of particle at 50 per cent point, microns
$Z$	"Plane of No Return" length, in.
$r$	Radius, in.
$V_t$	Tangential velocity, in. per sec.
$V_r$	Radial velocity, in. per sec.
$V_z$	Axial velocity, in. per sec.

$Q$	Total flow rate, cu. in. per sec.
$Q_u$	Underflow pot flow rate, cu. in. per sec.
$k'$	Constant for forced vortex expression
$k''$	Constant for free vortex expression
$C$	Constant for $d_{50}$ expressions (2-1) and (2-2)
$k$	Constant for flow capacity correlations (2-3), (2-4) and (2-5)
$D_o$	Diameter of overflow nozzle, in.
$D_f$	Diameter of inlet nozzle, in.
$D_c$	Diameter of hydroclone, in.
$\Delta P$	Differential pressure, lb. per sq. in.
$E$	Flow constant in equation (2-6)
$N$	Exponent for tangential velocity expression (4-21)
$N'$	Constant in equations (2-7) and (2-8)
$V_o$	Velocity of flow past sphere, in. per sec.
$\frac{dV_r}{dt}$	Radial acceleration, in. per sec. per sec.
$f(r)$	Function of $r$ , volts
$A$	Area, sq. in.
$U_1$	Negative velocity term in equation (4-17), in. per sec.
$Q_c$	Flow constant in equation (4-11)

$A_{iv}$	Area of inner vortex, sq. in.
$V_{iv}$	Velocity at inner vortex, in. per sec.
$V_i$	Velocity at inlet to hydroclone, in. per sec.
$A_i$	Area at inlet nozzle, sq. in.
$Q_{15}$	Flow rate for 15 gpm, cu. in. per sec.
$D_{10}$	Diameter of 10 micron particle, in.
$r_{0.25}$	Radius of 0.25 in. hydroclone, in.
A	Potentiometer in equation (4-27), dimensionless
B	Potentiometer in equation (4-28), dimensionless
C	Potentiometer in equation (4-29), dimensionless
$\pi$	Pi
$\mu$	Mu, Absolute viscosity, lb. force per sq. in.
$\rho_L$	Rho, Mass density of liquid, lb. mass per sq. in.
$\rho_S$	Rho, Mass density of solid, lb. mass per sq. in.
$\nu$	Nu, Kinematic viscosity, centistokes
$\phi$	Phi, Cone angle, degrees

## ABBREVIATIONS

lb	Pounds
cu	Cubic
sec	Seconds
psi	Pounds per square inch
sq	Square
in	Inch, inches
gpm	Gallons per minute

## APPENDIX C

The operation and principle of the particle counter was taken from Bulletin A-2 supplied by Coulter Electronics Incorporated.

The Coulter Counter determines the number and size of particles suspended in an electrically conductive liquid. The particles flow through a small aperture having an electrode on either side, with particle concentration such that the particles traverse the aperture substantially one at a time.

Each particle passage displaces electrolyte within the aperture, momentarily changing the resistance between the electrodes and producing a voltage pulse of magnitude proportional to particle volume. The resultant series of pulses is electronically amplified, scaled and counted.

The voltage pulses are displayed on the oscilloscope screen as a pattern of vertical "spikes". The pulse pattern serves as a guide for measurement and as a monitor of instrument performance. The pulses are also fed to a threshold circuit having an adjustable screen-out voltage level, and those pulses that reach or exceed this level are counted. Threshold level is indicated on the screen by a brightening of pulse segments above the threshold level.

Figure 17 is a schematic drawing of the Coulter Counter. When stopcock A is opened, a controlled external vacuum initiates flow from beaker A through the aperture, and unbalances the mercury manometer.

Closing stopcock A then isolates the system from the external vacuum, and the siphoning action of the rebalancing manometer continues the sample flow. The advancing mercury column activates the counter via start and stop probes, providing a count of the relative number of particles above a given range in a fixed volume of suspension.

The stopcock A is opened, the counter reset, and a fresh volume of fluid is drawn for another count. A series of counts from the sample beaker at various threshold settings provides direct data for different size particles.

Stopcock B and beaker B are used for flushing electrolyte through the aperture if it becomes choked with a particle that is larger than the aperture size.

The electrolyte that was used was made up of one part of 4 per cent lithium iodide in iso-propyl alcohol and one part ethylene dichloride. One part of Mil-O-spec 5606 hydraulic fluid and three parts of electrolyte were mixed for the solution to be used for the particle counter.



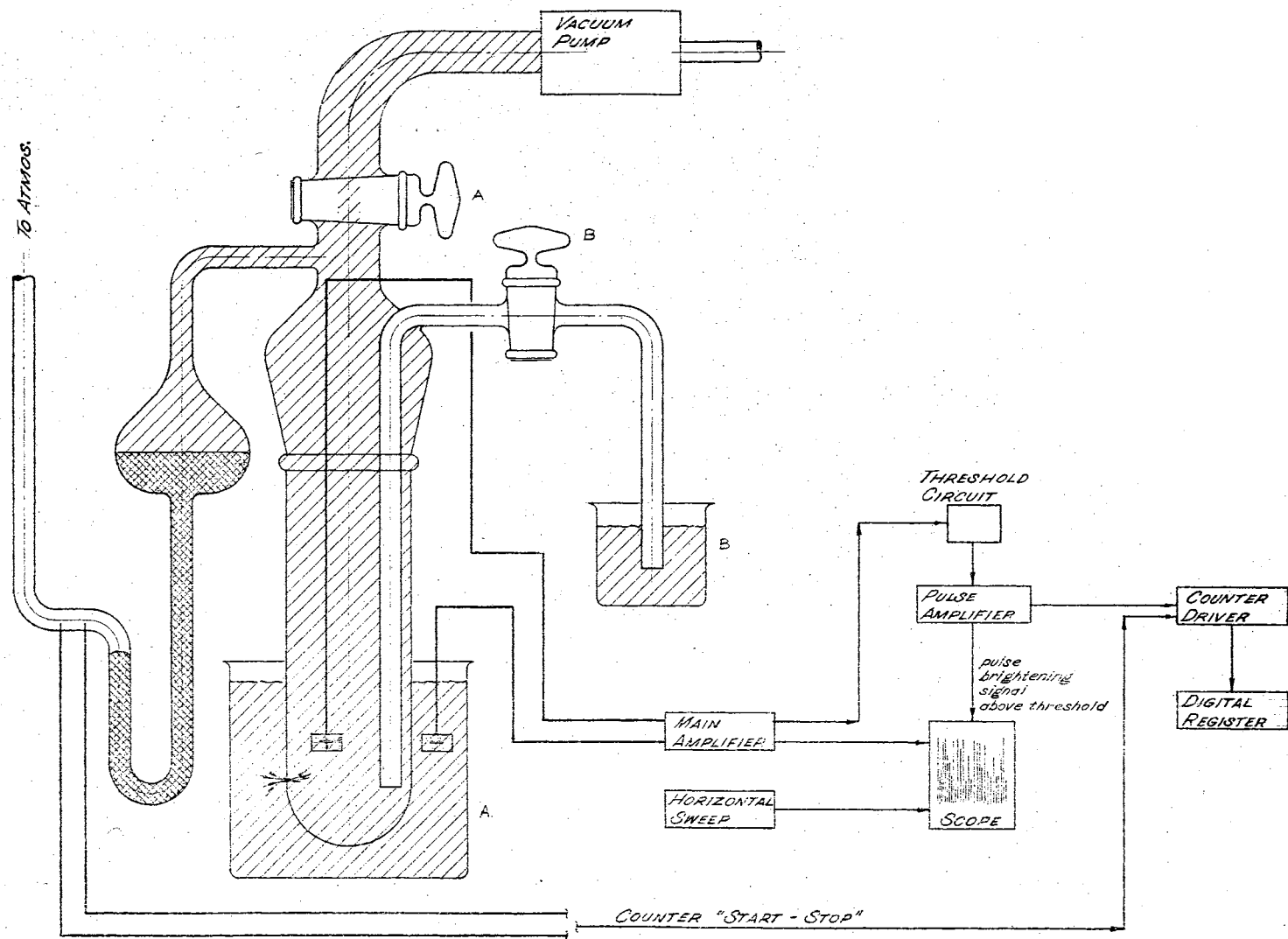


Figure 17. Coulter Counter Schematic

TABLE III

## COULTER COUNTER DATA

PARTICLE CONTAMINATION LABORATORY  
OKLAHOMA STATE UNIVERSITY  
Coulter Counter Data

Sample

Source

Electrolyte

Date 6-10-61

Aperture

Manometer

Coinc.

Calib.

Diameter 140M

Volume 2000 Ml

Factor p =

Factor k =

Dispersant

Oper

Aperture

Gain

Resistance

Index

NOTES 13.1 GPM 1.00 HYD DIA.

Threshold

F<sub>1</sub>

F<sub>2</sub>

F<sub>3</sub>

F<sub>4</sub>

F<sub>5</sub>

F<sub>6</sub>

F<sub>7</sub>

F<sub>8</sub>

F<sub>9</sub>

F<sub>10</sub>

Dial Expansion Factors

1.00

Aperture Current Selector Reading (I)

Particle Contaminant Diameter (d)

RAW COUNTS n'

Run 1

Run 2

Run 3

Average Count  $\bar{n}'$

Coincidence Correction  $n'' = \frac{(\bar{n}')^2}{1000}$

Full Count  $\bar{n} = \bar{n}' + n''$

Actual Count  $n = \bar{n}' - \text{background}$

Efficiency  $\eta\%$

Threshold Reading (t')

104

1

40

1

2

3

2

2

1

97.3

44

1

30

5

6

4

5

3

1

91.7

13

1

20

21

13

18

17

12

5

95.0

23.6

5

10

1176

1132

1148

1152

1135

1002

50.3

104

1

40

39

38

33

37

37

36

44

1

30

43

63

46

51

14

12

13

1

20

271

287

295

284

233

100

23.6

5

10

2377

2498

2428

2434

2150

2013

## APPENDIX D

### APPARATUS AND EQUIPMENT

1. Electrical Analog Computer: Manufacturer, Donner Scientific Company; Model 3400.
2. Hydraulic Power Unit: Model X-005 designed and built by School of Mechanical Engineering, Oklahoma State University.
3. Electronic Particle Counter: Manufacturer, Coulter Electronics Inc; Model A.

VITA

Robert Elwin Bose

Candidate for the Degree of  
Master of Science

Thesis: THE DEVELOPMENT OF AN EXPRESSION TO PREDICT THE  
MOVEMENT OF A PARTICLE IN A HYDROCLONE

Major Field: Mechanical Engineering

Biographical:

Personal Data: Born August 17, 1937, in Bessie,  
Oklahoma, the son of Edward and Margaret Bose.

Education: Graduated from Clinton High School,  
Clinton, Oklahoma, in May, 1955; received the  
degree of Bachelor of Science in Mechanical  
Engineering from Oklahoma State University,  
May, 1959; completed the requirements for the  
Master of Science degree in January, 1962.

Experience: Employed by Oklahoma State University  
from January, 1959 to September, 1961 as a  
Graduate Assistant.